



## OPEN ACCESS

## EDITED BY

Marc-Antoine Custaud,  
Université d'Angers, France

## REVIEWED BY

Shereen M. Hamza,  
University of Alberta, Canada  
Jamila H. Siamwala,  
Brown University, United States

## \*CORRESPONDENCE

Jeremy Rabineau,  
Jeremy.rabineau@ulb.be

## SPECIALTY SECTION

This article was submitted to  
Environmental, Aviation and  
Space Physiology,  
a section of the journal  
Frontiers in Physiology

RECEIVED 15 May 2022

ACCEPTED 13 September 2022

PUBLISHED 07 October 2022

## CITATION

Rabineau J, Issertine M, Hoffmann F,  
Gerlach D, Caiani EG, Haut B,  
van de Borne P, Tank J and Migeotte P-F  
(2022), Cardiovascular deconditioning  
and impact of artificial gravity during  
60-day head-down bed rest—Insights  
from 4D flow cardiac MRI.  
*Front. Physiol.* 13:944587.  
doi: 10.3389/fphys.2022.944587

## COPYRIGHT

© 2022 Rabineau, Issertine, Hoffmann,  
Gerlach, Caiani, Haut, van de Borne,  
Tank and Migeotte. This is an open-  
access article distributed under the  
terms of the [Creative Commons  
Attribution License \(CC BY\)](https://creativecommons.org/licenses/by/4.0/). The use,  
distribution or reproduction in other  
forums is permitted, provided the  
original author(s) and the copyright  
owner(s) are credited and that the  
original publication in this journal is  
cited, in accordance with accepted  
academic practice. No use, distribution  
or reproduction is permitted which does  
not comply with these terms.

# Cardiovascular deconditioning and impact of artificial gravity during 60-day head-down bed rest—Insights from 4D flow cardiac MRI

Jeremy Rabineau<sup>1,2\*</sup>, Margot Issertine<sup>1</sup>, Fabian Hoffmann<sup>3</sup>,  
Darius Gerlach<sup>3</sup>, Enrico G. Caiani<sup>4</sup>, Benoit Haut<sup>2</sup>,  
Philippe van de Borne<sup>1</sup>, Jens Tank<sup>3</sup> and  
Pierre-François Migeotte<sup>1</sup>

<sup>1</sup>LPHYS, Département de Cardiologie, Université Libre de Bruxelles, Brussels, Belgium, <sup>2</sup>TIPs, École Polytechnique de Bruxelles, Université Libre de Bruxelles, Brussels, Belgium, <sup>3</sup>Institute of Aerospace Medicine, German Aerospace Center (DLR), Cologne, Germany, <sup>4</sup>Electronic, Information and Biomedical Engineering Department, Politecnico di Milano, Milan, Italy

Microgravity has deleterious effects on the cardiovascular system. We evaluated some parameters of blood flow and vascular stiffness during 60 days of simulated microgravity in head-down tilt (HDT) bed rest. We also tested the hypothesis that daily exposure to 30 min of artificial gravity (1 g) would mitigate these adaptations. 24 healthy subjects (8 women) were evenly distributed in three groups: continuous artificial gravity, intermittent artificial gravity, or control. 4D flow cardiac MRI was acquired in horizontal position before (−9 days), during (5, 21, and 56 days), and after (+4 days) the HDT period. The false discovery rate was set at 0.05. The results are presented as median (first quartile; third quartile). No group or group × time differences were observed so the groups were combined. At the end of the HDT phase, we reported a decrease in the stroke volume allocated to the lower body (−30% [−35%; −22%]) and the upper body (−20% [−30%; +11%]), but in different proportions, reflected by an increased share of blood flow towards the upper body. The aortic pulse wave velocity increased (+16% [+9%; +25%]), and so did other markers of arterial stiffness (*CAVI*; *CAVI<sub>0</sub>*). In males, the time-averaged wall shear stress decreased (−13% [−17%; −5%]) and the relative residence time increased (+14% [+5%; +21%]), while these changes were not observed among females. Most of these parameters tended to or returned to baseline after 4 days of recovery. The effects of the artificial gravity countermeasure were not visible. We recommend increasing the load factor, the time of exposure, or combining it with physical exercise. The changes in blood flow confirmed the different adaptations occurring in the upper and lower body, with a larger share of blood volume dedicated to the upper body during (simulated) microgravity. The aorta appeared stiffer during the HDT phase, however all the changes remained subclinical and probably the sole consequence of reversible functional changes caused by reduced blood flow. Interestingly, some wall shear stress markers were more stable in females than

in males. No permanent cardiovascular adaptations following 60 days of HDT bed rest were observed.

#### KEYWORDS

bed rest, microgravity, artificial gravity, cardiac MRI, 4D flow, cardiovascular deconditioning, wall shear stress, pulse wave velocity

## Introduction

In microgravity as well as simulated microgravity, such as during head-down tilt (HDT) bed rest, a shift of blood volume from the lower to the upper body is observed (Shen and Frishman, 2019). It is then followed by a cascade of adaptations, including a decrease in plasma volume (Blomqvist and Stone, 1983). Together with hypokinesia, in the absence of proper countermeasures, long-term exposure to (simulated) microgravity leads to a decrease in stroke volume (Herault et al., 2000) and cardiac strain (Hoffmann et al., 2021), an increase in resting heart rate (HR) (Rabineau et al., 2020), and a post-flight orthostatic intolerance (Lee et al., 2015). On the vascular side, microgravity has also several deleterious effects (Navasiolava et al., 2020). However, current studies remain inconclusive regarding its exact impact on arterial stiffness, an important predictor of cardiovascular risk (Vlachopoulos et al., 2010). While some investigators observed an increased stiffness (Tuday et al., 2007; Hughson et al., 2016; Fayol et al., 2019; Hoffmann et al., 2022), others did not find any significant changes (Palombo et al., 2015; Hoffmann et al., 2019; Möstl et al., 2021).

The countermeasures currently used onboard the International Space Station appear to not optimally counteract the microgravity-induced deconditioning (Hargens et al., 2013; Hurst et al., 2019). Artificial gravity has been suggested as a multi-system countermeasure (Hargens et al., 2013) and is now studied in the context of HDT bed rest (Iwasaki et al., 2001; Iwase, 2005; Stenger et al., 2012). However, only basic investigations have been conducted so far and always for limited periods of exposure to (simulated) microgravity. As a consequence, not only longer studies are needed, but it is also necessary to evaluate the comparative efficacy of different protocols regarding the duration, intensity, and activity performed during exposure to artificial gravity (Hargens et al., 2013).

While assessing the cardiovascular state of an astronaut in space is operationally difficult, ground studies offer a relatively easy access to state-of-the-art technologies. Magnetic resonance imaging (MRI) is a good example of such a technology that can be available during HDT bed rest studies, but not in space. In particular, the recent advances in the field of cardiac MRI allow assessing many new parameters relevant to the cardiovascular health. For instance, 4D flow cardiac MRI can be used to provide a time-resolved 3D velocity field on a volume of interest during free breathing (Stankovic et al., 2014). Among others, this type of

protocol enables to accurately measure blood flow rates in the aorta (Houriez-Gombaudo-Saintonge et al., 2019). In turn, it allows the estimation of aortic pulse wave velocity (PWV) (Markl et al., 2012) and wall shear stress (WSS) (Stalder et al., 2008). Both are important markers of the vascular health (Takehara, 2022) and can help better understand the cardiovascular adaptations and potential risks for a subject exposed to a weightless environment.

Accordingly, the general objective of this research was to quantify the cardiovascular deconditioning induced by 60-day exposure to simulated microgravity by HDT bed rest, using 4D flow cardiac MRI. We expected to observe a decrease in the parameters of blood flow, leading to a decrease of aortic WSS and an increase in wall stiffness parameters such as aortic PWV. Additionally, the secondary objective was to evaluate the efficacy of a countermeasure based on artificial gravity, with the hypothesis that it would mitigate the changes in the previously cited parameters of the cardiovascular health, as compared to the control subjects.

## Materials and methods

### Study population and AGBRESA study

The research was part of the study “Artificial Gravity Bed Rest with European Space Agency” (AGBRESA) organized jointly by the American, European, and German space agencies (NASA, ESA, and DLR, respectively). It took place at the envihab facility of the DLR in Cologne, Germany, between March and December 2019. The AGBRESA study was approved by the Northern Rhine Medical Association (Ärztekammer Nordrhein, application N°2018143) as well as the Federal Office for Radiation Protection (Bundesamt für Strahlenschutz, application N°22464/2018-074-R-G). Written informed consent was obtained from all the subjects prior to starting the protocols.

Twenty-four healthy subjects (8 women) were included after a thorough medical screening (Kramer et al., 2021) (German Clinical Trials Register – DRKS00015677). They were randomly pre-assigned to three groups matched for sex, age, and weight: a continuous artificial gravity group (cAG,  $n = 8$ , 3 women), an intermittent artificial gravity group (iAG,  $n = 8$ , 3 women), or a control group (CTRL,  $n = 8$ , 2 women). Three subjects had to be discharged from the study for medical reasons that were not identified during the screening phase and that were not related to

**TABLE 1** Demographics of the subjects enrolled in the AGBRESA study at baseline (BDC-9). Data are presented as median (first quartile; third quartile), except for the number of subjects (number of females in parentheses). cAG: continuous artificial gravity; iAG: intermittent artificial gravity; CTRL: control.

Group	All	cAG	iAG	CTRL
# subjects (females)	24 (8)	8 (3)	8 (3)	8 (2)
Age (years)	29 (26; 38)	29 (25; 34)	27 (26; 44)	33 (27; 41)
Body mass (kg)	74 (70; 80)	74 (65; 76)	72 (67; 75)	80 (74; 88)
Body height (cm)	176 (167; 182)	175 (165; 176)	175 (163; 184)	179 (173; 183)

the study protocol. These three subjects have been replaced and the demographics of the final study population can be found in [Table 1](#).

Each subject started with a 14-day baseline data collection (BDC) period before being assigned to one of the three aforementioned groups. Then, they began a 60-day strict (i.e., without a pillow under the head)  $-6^\circ$  HDT bed rest period, which was followed by a 14-day recovery (R) period. While the subjects were continuously monitored to remain in HDT position during the whole HDT phase, they were authorized to move freely within the ward during the BDC and R phases. Daily water and energy intakes were standardized and controlled throughout the study. The female subjects did not take oral contraceptives and their menstrual cycle was not controlled for. A few subjects experienced some discomfort, especially at the beginning of the HDT phase, including headache, stuffy nose, and back pain. However, these symptoms were never judged as clinically significant, and we believe that they did not impact the results presented thereafter. Additional details regarding the whole protocol are also given in ([Kramer et al., 2021](#)).

During the HDT phase, the cAG and iAG groups underwent daily 30-minute exposure to artificial gravity in horizontal ( $0^\circ$ ) position, using the short-arm human centrifuge available at: envihab. The position of the subject and rotation speed were adapted on an individual basis to achieve a head-to-foot acceleration of 1 g at the center of mass and 2 g at the feet. The cAG group underwent single continuous 30-minute runs on the centrifuge, while, in the iAG group, these 30 min of daily exposure to artificial gravity were distributed in 6 bouts of 5 min separated by 3-minute breaks. The CTRL group was not exposed to artificial gravity during the whole HDT phase. Additional details regarding the artificial gravity protocol, including average spin rate and radii, can be found in ([Frett et al., 2020b](#)) and ([Kramer et al., 2021](#)).

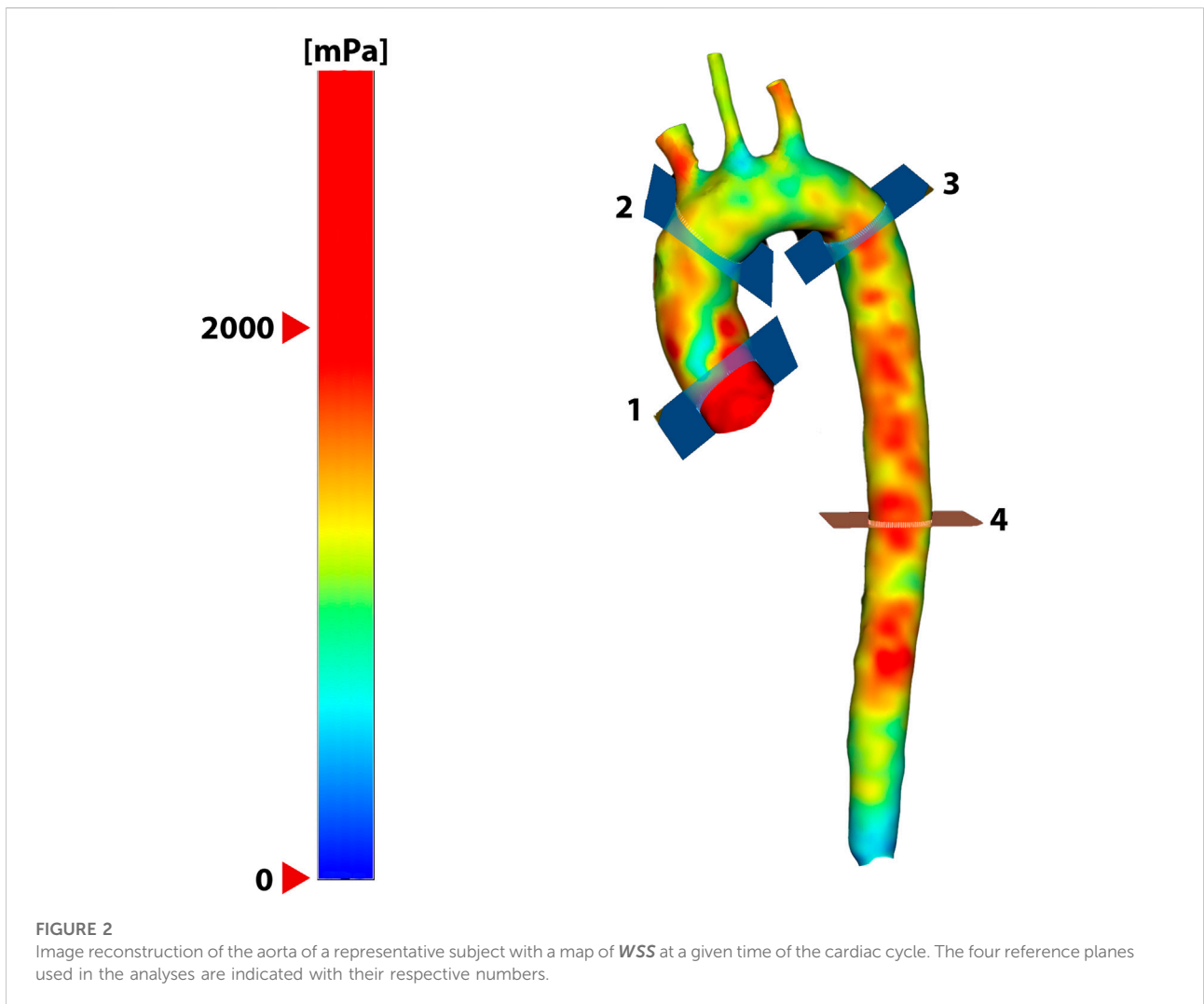
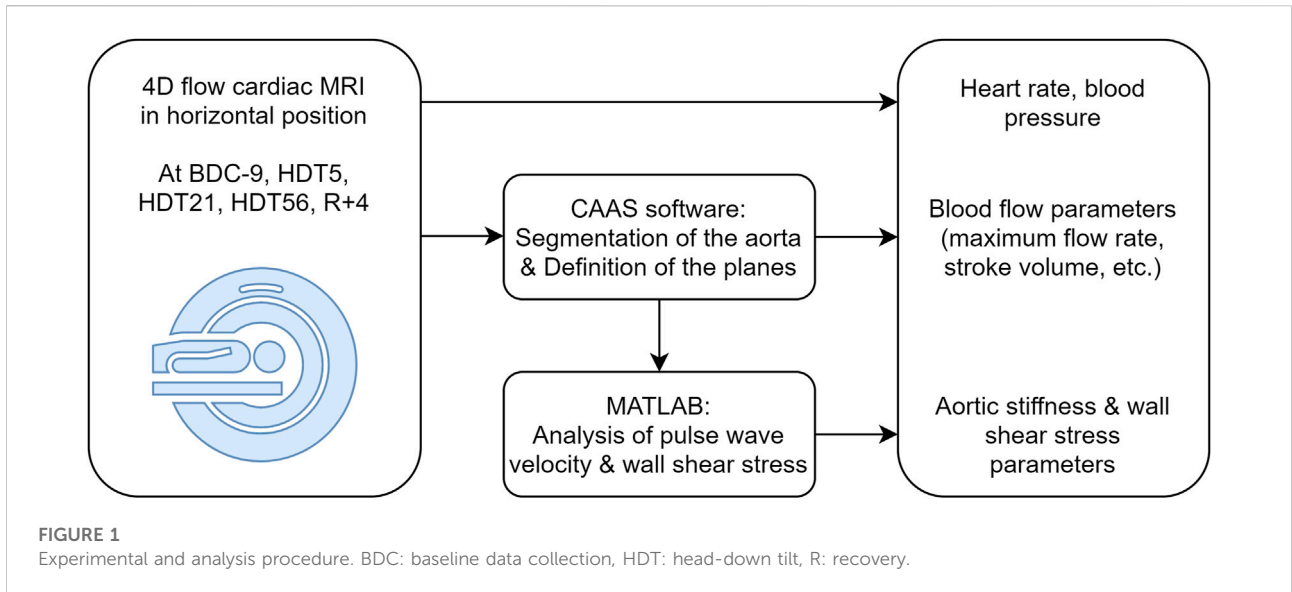
## 4D flow cardiac MRI

The cardiac MRI image acquisition was performed using a Biograph mMR 3-T scanner (Siemens, Erlangen, Germany) with the subject in supine position and no use of contrast agents. The

same procedure was repeated at several time points all along the study: before ( $-9$  days, written BDC-9), after ( $+4$  days, written R+4), and during the HDT phase (5, 21, and 56 days, written HDT5, HDT21, and HDT56, respectively). Five subjects had to perform the R+4 data point slightly later (four at  $+6$  days and one at  $+5$  days after the HDT phase) for operational reasons. The cardiac MRI protocol included a free breathing 4D flow acquisition with prospective electrocardiogram- and navigator-gating in a volume encompassing the thoracic aorta. A three-directional encoding velocity of 150 cm/s and the acquisition of 20 images per cardiac cycle were chosen, together with the following parameters: voxel size,  $2.375 \times 2.375 \times 2.00$  mm<sup>3</sup>; repetition time, 38.72 ms; echo time, 2.29 ms; flip angle,  $7^\circ$ ; acquisition matrix,  $90 \times 160$ ; and number of slices, 40. In addition, blood pressure at the right brachial artery was measured (Expression MR400, Philips Healthcare, Eindhoven, Netherlands) during the cardiac MRI protocol, a few minutes before the 4D flow acquisition. This protocol is summarized in [Figure 1](#) together with the steps of the analysis.

The post-hoc analysis of the 4D flow images was performed using CAAS MR Solutions 5.2.1 (Pie Medical Imaging BV, Maastricht, The Netherlands) and MATLAB R2018b (The MathWorks, Inc., Natick, Massachusetts, United States). During the pre-processing step, the background phase offsets and velocity aliasing were automatically corrected, as recommended ([Dyverfeldt et al., 2015](#)). Then, the aortic volume was semi-automatically segmented and the centerline was extracted using the built-in functionalities available in the commercial software. Four planes were then positioned perpendicularly to the aortic centerline at standardized anatomical landmarks ([van Hout et al., 2020](#)) ([Figure 2](#)): 1.0 cm after the sinotubular junction (plane 1), just proximal to the brachiocephalic artery (plane 2), 2.0 cm distal to the left subclavian artery (plane 3), and 10.0 cm distal to plane 3 (plane 4).

The total stroke volume ( $SV_{tot}$ ) was defined as the total amount of blood passing through the plane 2 in one cardiac cycle, while the total amount of blood passing through the plane 3 in one cardiac cycle was considered as the stroke volume allocated to the lower body ( $SV_{low}$ ). The stroke volume allocated to the upper body ( $SV_{up}$ ) was then computed as the difference between  $SV_{tot}$  and  $SV_{low}$ . The mean HR measured during the 4D flow



protocol was used to convert these values in terms of cardiac output ( $CO_{tot}$ ,  $CO_{low}$ , and  $CO_{up}$ , respectively). Based on these values, we then computed the percentage of the cardiac output allocated to the upper body ( $\%CO_{up}$ ).

The maximum blood flow rate in the ascending aorta ( $Q_{max,AA}$ ) was measured on plane 2, while the one in the descending aorta ( $Q_{max,DA}$ ) was measured on plane 3.

The systemic vascular resistance (SVR) was calculated as the ratio of the mean arterial pressure to the cardiac output, according to the following formula (Lee et al., 2020):

$$SVR = \frac{SBP + 2 DBP}{3} \frac{1}{CO_{tot}} \quad (1)$$

with  $SBP$  and  $DBP$  the systolic and diastolic blood pressures, respectively.

The total arterial compliance ( $TAC$ ) was calculated as the ratio of  $SV_{tot}$  to the pulse pressure (Lee et al., 2020):

$$TAC = \frac{SV_{tot}}{SBP - DBP} \quad (2)$$

The aortic pulse wave velocity ( $PWV$ ) was measured between planes 1 and 4. To do so, intermediate planes were defined every 0.6 cm along the centerline, for a total number of  $35 \pm 2$  planes. The associated mean velocity curves were interpolated with a time step of 1 ms using a spline function. A frequency domain method was then used to estimate the pulse transit time ( $PTT$ ) through these planes. To do so, the mean velocity curves were normalized, before their Fourier transforms were computed. Then, the filter transfer function  $H$  was derived:

$$H(f) = \frac{Y(f)}{X(f)} \quad (3)$$

with  $X(f)$  and  $Y(f)$  the Fourier transforms of the normalized mean velocity curves for the two planes of interest, evaluated at frequency  $f$ .

The  $PTT$  between these two planes was then given as the sum of the filter group delay weighted by the harmonics of the input signal (Meloni et al., 2014):

$$PTT = \sum_f - \frac{d\varphi(H(f))}{df} \frac{|X(f)|^2}{2\pi \sum_f |X(f)|^2} \quad (4)$$

with  $\varphi(H(f))$  the phase of the filter  $H(f)$ .

This procedure was applied to compute  $PTT$  between plane 1 and each intermediate plane until plane 4. The values of  $PTT$  as a function of the distance with plane 1 populated a scatter plot, on which a linear fit was performed using the least squares method. Finally, the  $PWV$  was given by the reciprocal of the slope of the fitted line.

We also computed the cardio-ankle vascular index ( $CAVI$ ) and an updated version of this index ( $CAVI_0$ ), using the following formulas:

$$CAVI = \frac{2\rho}{SBP - DBP} \ln\left(\frac{SBP}{DBP}\right) PWV^2 \quad (5)$$

with  $PWV$  measured in m/s,  $SBP$  and  $DBP$  measured in Pa, and  $\rho = 1050 \text{ kg/m}^3$  the volumetric mass density of blood (Pedley, 1980).

$$CAVI_0 = 2\rho \frac{PWV^2}{DBP} - \ln\left(\frac{DBP}{P_0}\right) \quad (6)$$

with  $P_0 = 13332 \text{ Pa}$  (corresponding to 100 mmHg) a reference pressure equal to the one commonly used in the literature (Giudici et al., 2021).

The intersection between the segmented aorta and each of the four planes previously defined was performed automatically, before extrapolating to the point of zero velocity to properly locate the aortic wall. Assuming a constant blood viscosity of 4.0 mPa.s, the  $WSS$  vector was then computed on 90 wall points for each of these planes, as in (Demir et al., 2022). On a given plane, the average of all these 90  $WSS$  amplitudes during the peak systolic phase was defined as  $WSS_{mean}$ , and the time-averaged  $WSS$  over the cardiac cycle as  $TAWSS$ . The  $WSS$  fluctuations were also evaluated using the oscillatory shear index  $OSI$  (Callaghan and Grieve, 2018):

$$OSI = \frac{1}{2} \left( 1 - \frac{\left\| \int_0^T \mathbf{WSS}(t) dt \right\|}{\int_0^T \|\mathbf{WSS}(t)\| dt} \right) \quad (7)$$

with  $T$  the average cardiac cycle duration and  $t$  the time.

The relative residence time ( $RRT$ ) was computed based on the following equation (Rikhtegar et al., 2012):

$$RRT \sim \frac{1}{TAWSS (1 - 2 OSI)} \quad (8)$$

where the proportionality constant between  $RRT$  and the right-hand side of the expression can be chosen arbitrarily (here it was set to  $10^3$ ).

For the sake of simplicity, in this paper, only the  $WSS$  results in the ascending aorta (plane 2) are presented. However, the results in the other planes are similar.

## Statistical analysis

The statistical analysis was performed using GraphPad Prism 9.1.2 (GraphPad Software, San Diego, CA, United States). Three records from two distinct subjects of the CTRL group could not be considered in the analysis due to poor data quality. The effects of time, group, and sex were assessed using a mixed-effects model with the Geisser-Greenhouse correction. If no group and no group  $\times$  time differences were observed for the metrics studied, the subjects were pooled into a single group of 24 subjects. When the mixed-effects model displayed a significant effect of time, multiple comparisons

**TABLE 2** Evolution of blood flow results in the ascending and the descending aorta (AA and DA, respectively) all over the study. Data are presented as median (first quartile; third quartile). The group  $\times$  time and sex  $\times$  time effects are displayed in the last columns. *HR*: heart rate, *Q<sub>max</sub>*: maximum blood flow rate, *SV<sub>tot</sub>*: total stroke volume, *SV<sub>low</sub>*: stroke volume allocated to the lower body, *SV<sub>up</sub>*: stroke volume allocated to the upper body. Their equivalent in terms of cardiac output is noted *CO<sub>tot</sub>*, *CO<sub>low</sub>*, and *CO<sub>up</sub>*, respectively. %*CO<sub>up</sub>*: percentage of cardiac output allocated to the upper body. *SVR*: systemic vascular resistance. BDC: baseline data collection, HDT: head-down tilt, R: recovery. \*: Significant difference with BDC-9 using the two-stage linear step-up procedure of Benjamini, Krieger, and Yekutieli with a false discovery rate set at 0.05.

	BDC-9	HDT5	HDT21	HDT56	R+4	group $\times$ time effect	sex $\times$ time effect
<i>HR</i> (bpm)	56 (52; 67)	56 (54; 66)	60 (51; 70)	61 (57; 72) *	65 (57; 73) *	$p = 0.68$	$p = 0.80$
<i>Q<sub>max,AA</sub></i> (ml/s)	444 (356; 512)	387 (351; 473) *	399 (330; 471) *	426 (327; 456) *	412 (374; 491) *	$p = 0.88$	$p = 0.51$
<i>Q<sub>max,DA</sub></i> (ml/s)	311 (256; 341)	265 (222; 308) *	260 (217; 311) *	258 (201; 315) *	294 (235; 322) *	$p = 0.46$	$p = 0.16$
<i>SV<sub>tot</sub></i> (ml)	89 (78; 106)	76 (62; 83) *	73 (57; 84) *	73 (58; 79) *	85 (73; 108)	$p = 0.85$	$p = 0.22$
<i>SV<sub>low</sub></i> (ml)	63 (50; 68)	50 (36; 56) *	44 (36; 52) *	43 (34; 53) *	57 (45; 65) *	$p = 0.59$	$p = 0.30$
<i>SV<sub>up</sub></i> (ml)	27 (25; 38)	25 (22; 31)	27 (22; 32)	27 (20; 32) *	31 (25; 40)	$p = 0.29$	$p = 0.19$
<i>CO<sub>tot</sub></i> (l/min)	5.0 (4.7; 5.6)	4.3 (3.9; 4.7) *	4.1 (3.8; 4.7) *	4.4 (3.8; 4.7) *	5.7 (4.8; 6.2) *	$p = 0.65$	$p = 0.19$
<i>CO<sub>low</sub></i> (l/min)	3.3 (3.2; 3.7)	2.8 (2.4; 3.0) *	2.5 (2.2; 3.1) *	2.7 (2.1; 3.1) *	3.6 (3.0; 4.0)	$p = 0.28$	$p = 0.30$
<i>CO<sub>up</sub></i> (l/min)	1.7 (1.3; 2.2)	1.6 (1.3; 1.8)	1.6 (1.5; 1.7)	1.7 (1.4; 1.9)	2.1 (1.7; 2.4) *	$p = 0.27$	$p = 0.15$
% <i>CO<sub>up</sub></i> (%)	34 (29; 40)	37 (32; 41) *	38 (34; 41) *	40 (33; 43) *	37 (34; 39) *	$p = 0.07$	$p = 0.19$
<i>SVR</i> (mmHg.min/l)	16.0 (14.8; 17.7)	20.8 (18.4; 23.4) *	20.5 (18.2; 23.8) *	20.3 (18.9; 23.8) *	14.2 (13.1; 16.9) *	$p = 0.42$	$p = 0.24$

**TABLE 3** Evolution of blood pressure and arterial stiffness results computed between planes 1 and 4 (Figure 2) all over the study. Data are presented as median (first quartile; third quartile). The group  $\times$  time and sex  $\times$  time effects are displayed in the last columns. *TAC*: total arterial compliance, *PWV*: pulse wave velocity, *CAVI*: cardio-ankle vascular index, *CAVI<sub>0</sub>*: updated cardio-ankle vascular index, *DBP* and *SBP*: diastolic and systolic blood pressure, respectively, BDC: baseline data collection, HDT: head-down tilt, R: recovery. \*: Significant difference with BDC-9 using the two-stage linear step-up procedure of Benjamini, Krieger, and Yekutieli with a false discovery rate set at 0.05.

	BDC-9	HDT5	HDT21	HDT56	R + 4	group $\times$ time effect	sex $\times$ time effect
<i>TAC</i> (ml/mmHg)	1.51 (1.41; 1.87)	1.49 (1.19; 1.62) *	1.41 (1.24; 1.57) *	1.32 (1.08; 1.45) *	1.65 (1.48; 1.84) *	$p = 0.13$	$p = 0.57$
<i>PWV</i> (m/s)	5.3 (4.9; 6.0)	5.9 (5.2; 6.8) *	6.0 (5.2; 7.1) *	6.2 (5.5; 6.9) *	5.2 (4.3; 6.1)	$p = 0.49$	$p = 0.89$
<i>CAVI</i>	5.2 (4.1; 6.2)	5.8 (4.4; 8.2) *	5.8 (4.5; 8.3) *	6.3 (5.0; 9.1) *	5.1 (3.5; 6.5)	$p = 0.67$	$p = 0.88$
<i>CAVI<sub>0</sub></i>	7.9 (5.9; 9.2)	8.1 (6.4; 11.4) *	8.1 (6.4; 11.3) *	8.6 (6.6; 12.8) *	6.9 (4.9; 9.5)	$p = 0.42$	$p = 0.89$
<i>DBP</i> (mmHg)	66 (60; 68)	74 (68; 77) *	71 (68; 76) *	70 (68; 75) *	67 (62; 67)	$p = 0.51$	$p = 0.72$
<i>SBP</i> (mmHg)	120 (114; 124)	123 (114; 132) *	126 (115; 131) *	123 (116; 131) *	115 (110; 122) *	$p = 0.61$	$p = 0.98$

were performed using the two-stage linear step-up procedure of Benjamini, Krieger, and Yekutieli (Benjamini et al., 2006) to compare each time point to BDC-9. The false discovery rate was set at 0.05. The results are presented as median (first quartile; third quartile), unless otherwise stated. In particular, the relative differences between different conditions are computed based on individual relative differences, before extracting the corresponding quantiles (median and quartiles).

## Results

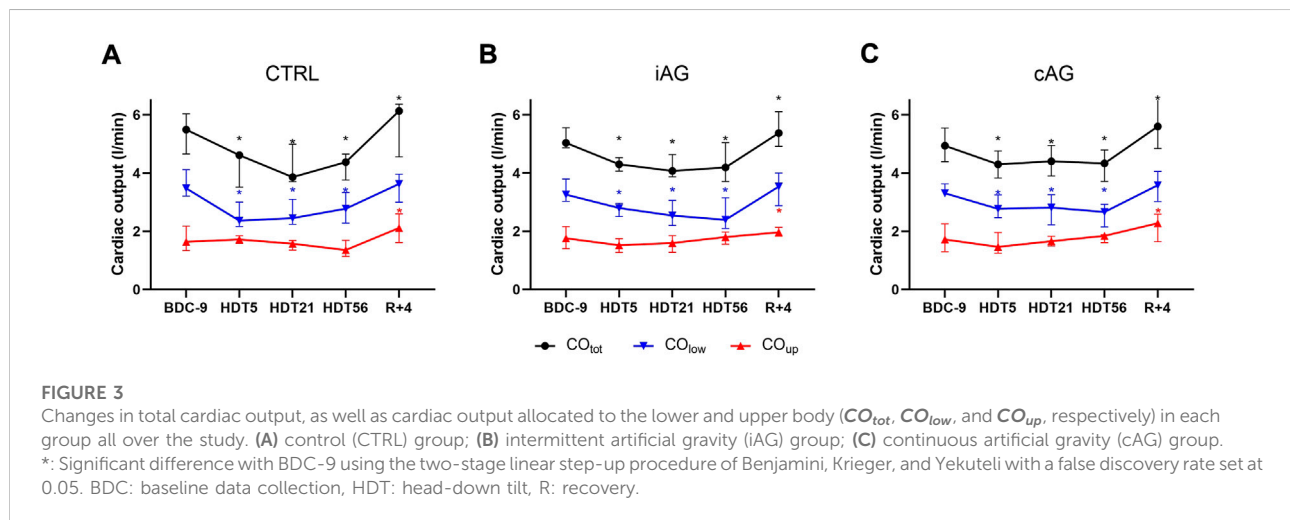
No group, group  $\times$  time, group  $\times$  sex, and group  $\times$  sex  $\times$  time differences were found at any time point and for any reported

feature. The  $p$  values corresponding to the group  $\times$  time effect are given in the penultimate column of Table 2 column of for the blood flow metrics, of Table 3 for the arterial stiffness metrics, and of Table 4 for the WSS metrics. The data from the three groups were then pooled. All the results presented hereafter correspond to the whole set of 24 subjects.

The results related to *HR*, *Q<sub>max</sub>*, *SV*, *CO*, and *SVR* are reported in Table 2. The resting *HR* was stable during the beginning of the HDT phase and increased only at HDT56 (+8% [+1%; +15%],  $p < 0.001$ ) and at R+4 (+7% [+3%; +15%],  $p < 0.001$ ), when compared to baseline values. In parallel, the peak flow rates in both the ascending and descending aorta decreased at all time points (with -9% [-16%; -2%] in the ascending aorta and -16% [-21%; -5%]

**TABLE 4** Evolution of wall shear stress results computed in the ascending aorta (plane 2, **Figure 2**) all over the study. Data are presented as median (first quartile; third quartile). The group  $\times$  time and sex  $\times$  time effects are displayed in the last columns.  $WSS_{mean}$ : average amplitude of all the  $WSS$  reference points during the peak systolic phase,  $TAWSS$ : time-averaged wall shear stress,  $OSI$ : oscillatory shear index,  $RRT$ : relative residence time, BDC: baseline data collection, HDT: head-down tilt, R: recovery. \*: Significant difference with BDC-9 using the two-stage linear step-up procedure of Benjamini, Krieger, and Yekutieli with a false discovery rate set at 0.05.

	BDC-9	HDT5	HDT21	HDT56	R + 4	group $\times$ time effect	sex $\times$ time effect
$WSS_{mean}$ (mPa)	1331 (1063; 1471)	1165 (1045; 1368) *	1213 (1008; 1293) *	1175 (1005; 1399) *	1299 (1207; 1492)	$p = 0.73$	$p = 0.46$
$TAWSS$ (mPa)	470 (416; 509)	429 (379; 463) *	417 (382; 431) *	405 (386; 437) *	476 (437; 515)	$p = 0.37$	$p = 0.04$
$OSI$ ( $\times 10^{-2}$ )	3.28 (2.81; 3.77)	3.21 (2.94; 3.79)	3.24 (2.90; 3.67)	3.24 (2.96; 3.59)	3.21 (2.86; 3.56)	$p = 0.93$	$p = 0.43$
$RRT$	2.3 (2.1; 2.6)	2.5 (2.3; 2.8) *	2.6 (2.5; 2.8) *	2.6 (2.5; 2.8) *	2.3 (2.1; 2.5)	$p = 0.57$	$p = 0.04$



in the descending aorta at HDT56 vs. BDC-9, both  $p < 0.001$ ). The values of  $SV_{tot}$ ,  $SV_{low}$ , and  $SV_{up}$  decreased at HDT56 vs. BDC-9 ( $-23\%$  [ $-33\%$ ;  $-16\%$ ],  $p < 0.001$ ;  $-30\%$  [ $-35\%$ ;  $-22\%$ ],  $p < 0.001$ ; and  $-20\%$  [ $-30\%$ ;  $+11\%$ ],  $p = 0.03$ , respectively). For  $SV_{tot}$  and  $SV_{low}$ , a smaller ( $p < 0.01$ ) decrease was observed as early as HDT5 ( $-17\%$  [ $-23\%$ ;  $-8\%$ ] and  $-21\%$  [ $-29\%$ ;  $-14\%$ ], respectively, both  $p < 0.001$ ). In the case of  $SV_{low}$ , it even persisted until R+4 ( $-7\%$  [ $-14\%$ ;  $+1\%$ ],  $p = 0.03$ ). When converting this information in terms of cardiac output, it appears that  $CO_{up}$  remained unchanged during the whole HDT phase, and even slightly increased at R+4, compared to BDC-9 ( $+21\%$  [ $-5\%$ ;  $+40\%$ ],  $p = 0.009$ ). In contrast,  $CO_{tot}$  and  $CO_{low}$  followed the same evolution as  $SV_{tot}$  and  $SV_{low}$  during the HDT phase. These different trends are visible in **Figure 3** and induce changes in  $\%CO_{up}$ , which is higher than baseline during the whole HDT phase ( $40\%$  [ $33\%$ ;  $43\%$ ] at HDT56 versus  $34\%$  [ $29\%$ ;  $40\%$ ] at BDC-9,  $p = 0.007$ ) and still at R+4 ( $37\%$  [ $34\%$ ;  $39\%$ ],  $p = 0.03$ ).  $SVR$  was also higher than baseline during the whole HDT phase ( $+34\%$  [ $+12\%$ ;  $+52\%$ ] at HDT56,  $p < 0.001$ ), but it decreased at R+4 ( $-7\%$  [ $-16\%$ ;  $+3\%$ ],  $p = 0.006$ ).

The results relevant to blood pressure and arterial stiffness are reported in **Table 3**. Compared to baseline values, both  $SBP$  and  $DBP$  increased during the HDT phase (e.g., at HDT56:  $+2\%$  [ $+0\%$ ;  $+6\%$ ],  $p < 0.001$  for  $SBP$ , and  $+11\%$  [ $+6\%$ ;  $+17\%$ ],  $p = 0.01$  for  $DBP$ ), while  $TAC$  decreased ( $-20\%$  [ $-12\%$ ;  $-2\%$ ] at HDT56,  $p < 0.001$ ).  $PWV$  was higher than baseline at all time points of the HDT phase ( $+16\%$  [ $+9\%$ ;  $+25\%$ ] at HDT56,  $p < 0.001$ ). This was also the case of the two corrected markers based on  $PWV$ :  $CAVI$  ( $+23\%$  [ $+12\%$ ;  $+55\%$ ] at HDT56,  $p = 0.001$ ) and  $CAVI_0$  ( $+15\%$  [ $+4\%$ ;  $+45\%$ ] at HDT56,  $p = 0.006$ ). For all these parameters, the changes disappeared quickly during the recovery phase, with even an overshoot at R+4 for  $SBP$  ( $-5\%$  [ $-6\%$ ;  $-2\%$ ],  $p = 0.01$ ) and  $TAC$  ( $+2\%$  [ $-2\%$ ;  $+14\%$ ],  $p = 0.007$ ).

**Table 4** summarizes the results relevant to  $WSS$ . Both markers of  $WSS$  amplitude decreased during the whole HDT phase and came back to baseline values as early as R+4. At HDT56, this decrease reached  $-5\%$  ( $-10\%$ ;  $-1\%$ ) ( $p = 0.02$ ) for  $WSS_{mean}$  and  $-11\%$  ( $-17\%$ ;  $-4\%$ ) ( $p < 0.001$ ) for  $TAWSS$ . In contrast,  $OSI$  was left relatively unaffected during the whole study ( $p = 0.78$ ).  $RRT$  increased during the whole HDT phase ( $+11\%$  [ $+4\%$ ;  $+21\%$ ] at

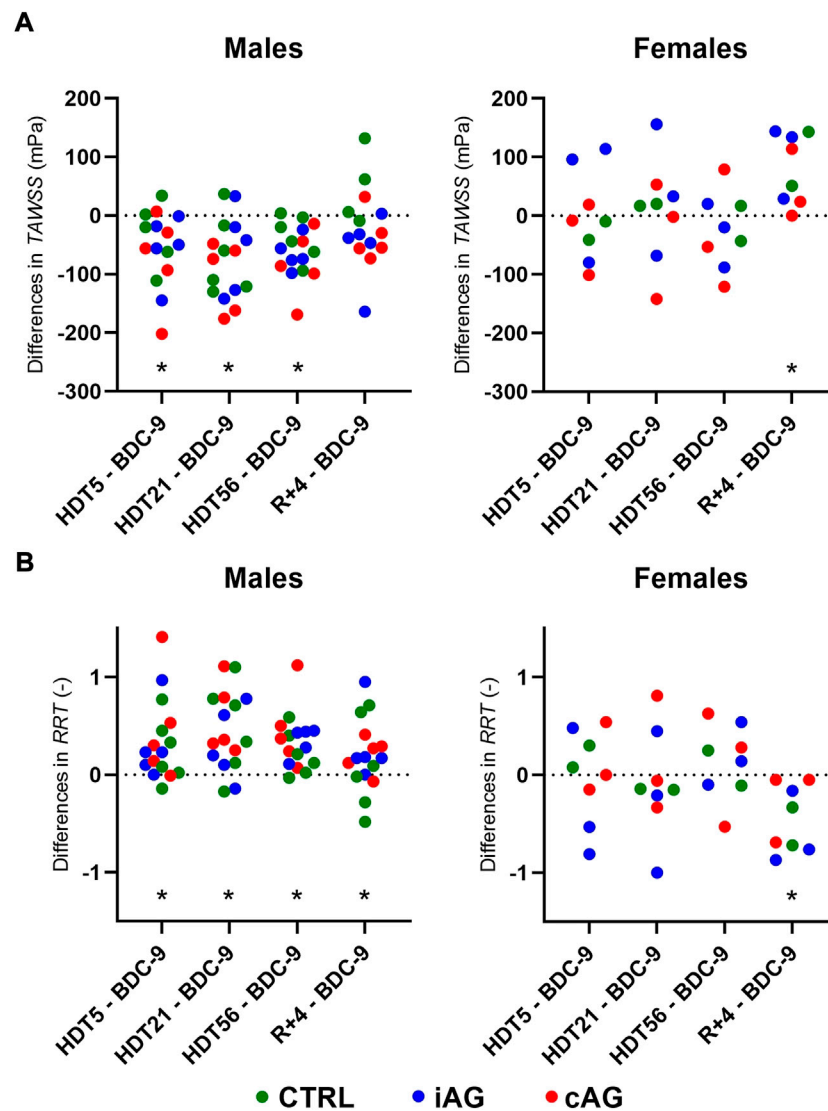


FIGURE 4

Individual evolution of: (A) *TAWSS* and (B) *RRT* among males and females and in each group at different timepoints, compared to their baseline values. \*: Significant difference with BDC-9 using the two-stage linear step-up procedure of Benjamini, Krieger, and Yekutieli with a false discovery rate set at 0.05. cAG: continuous artificial gravity, iAG: intermittent artificial gravity, CTRL: control, BDC: baseline data collection, HDT: head-down tilt, R: recovery.

HDT56 vs. BDC-9,  $p < 0.001$ ) with, again, a quick return to baseline values at R+4.

The last columns of Table 2, Table 3, and Table 4 present the sex  $\times$  time effects for the flow, stiffness, and WSS markers, respectively. The only markers presenting a significant sex  $\times$  time effect are related to WSS: *TAWSS* and *RRT* (both  $p = 0.04$ ). The impact of sex on the evolution of *TAWSS* and *RRT* during the HDT bed rest study is further depicted in Figure 4, where each timepoint is compared to its baseline value. During the HDT phase, the decrease in *TAWSS* was observed in males ( $-13\%$  [ $-17\%$ ;  $-5\%$ ] at HDT56 vs. BDC-9,  $p < 0.001$ ) but not in females. At R+4, *TAWSS* was back to baseline values in males, while it was increased in females ( $+13\%$

[ $+6\%$ ;  $+35\%$ ],  $p = 0.007$ ). As for *RRT*, the increase was observed in males during the HDT phase ( $+14\%$  [ $+5\%$ ;  $+21\%$ ] at HDT56 vs. BDC-9,  $p < 0.001$ ), while it seemed preserved in females. At R+4, it was still higher than baseline in males, while in females it was decreased ( $-18\%$  [ $-27\%$ ;  $-6\%$ ],  $p = 0.007$ ).

## Discussion

We used 4D flow cardiac MRI to assess cardiovascular deconditioning among subjects exposed to 60-day strict HDT bed rest. This technique allowed the evaluation of many

parameters based on the acquisition of a single volume of interest. The absence of significant differences between the three groups of subjects shows the lack of efficacy of the artificial gravity countermeasure on the estimated parameters. In addition to previously known results relevant to blood flow in (simulated) microgravity, our study confirmed that the cardiac output allocated to the upper and the lower body was differently affected. An increase in several markers of arterial stiffness was observed during the whole HDT phase, with a quick return to baseline values during the recovery phase. The markers related to WSS amplitude decreased during the HDT phase, while *RRT* increased. All of them were also back to baseline values shortly during the recovery period. Interestingly, the *TAWSS* and *RRT* changes were visible only among men during HDT, with opposite changes occurred among women during recovery.

These findings could not only be relevant for astronauts, but also for patients forced to prolonged bedridden immobilization. Indeed, both populations suffer from a multi-system deconditioning that requires to be better understood to find effective countermeasures. In fact, it has been shown that the changes in blood distribution may contribute to the observed bone loss (Colleran et al., 2000), while the arterial adaptations contribute to orthostatic intolerance (Delp, 2007), which can lead to falls and fall-related injuries.

## Interest of 4D flow

4D flow cardiac MRI allows for a very comprehensive assessment of blood flow dynamics in a pre-defined 3D volume throughout the cardiac cycle. Analysis planes can be placed retrospectively at any location within the acquisition volume. Not only does this allow to perform quality checks of the internal consistency of the data (Wentland et al., 2013), but it can also prevent using several standard 2D cine phase contrast protocols, each requiring accurate positioning of the relevant plane while the subject is lying in the scanner. Even though the scanning time of a 4D flow cardiac MRI protocol is longer than the one of a single 2D cine phase contrast acquisition, it can become advantageous in case a series of 2D acquisitions must be scanned (Dyverfeldt et al., 2015). This is especially important in HDT bed rest studies like this one, since it is not desired to ask subjects to remain in horizontal position for too long, especially during the HDT phase, to avoid physiological changes moving from  $-6^\circ$  to  $0^\circ$  position. Nevertheless, the measurements are limited to physiological steady state situations.

In addition to the sole blood flow and its traditional metrics, the analysis of the 4D flow images allows the computation of additional parameters, such as the one presented in Table 2 and Table 3. To properly assess *PWV*, an average of 35 planes all along the aorta were retrospectively defined, which would not have been feasible with 2D cine phase contrast. Other authors have already shown that the evaluation of *PWV* based on a small

number of planes results in less accurate measures (Houriez-Gombaud-Saintonge et al., 2019). Here we used a frequency method because, together with time-frequency methods, they are the most robust to low temporal resolutions (Houriez-Gombaud-Saintonge et al., 2019), correlate well with the traditional carotid-femoral *PTT* (Bargiotas et al., 2015), and show few outliers (Harloff et al., 2018). Besides this, the distance between each plane can be accurately measured, which is generally not the case for other methods measuring *PWV*. Finally, 4D flow cardiac MRI image acquisition is performed with the subjects in free breathing, as opposed to traditional acquisitions in breath hold. It is thus more representative of the normal cardiovascular state of the subjects.

## Interest of artificial gravity as a countermeasure

The absence of any visible efficacy of the countermeasure used in this study is not very surprising. Indeed, it is in line with other investigations conducted with the same subjects during the same study, showing its inefficacy: to maintain aerobic exercise capacity (Kramer et al., 2021), to limit the cardiac adaptations (Hoffmann et al., 2021), and to show benefits on the vascular system (Möstl et al., 2021). A 5-day HDT bed rest study with similar artificial gravity parameters (head-to-foot acceleration of 1 g at the center of mass during 30 min per day, continuous or intermittent) led to similar conclusions, with no effect of the countermeasure on plasma volume and aerobic power (Linnarsson et al., 2015), as well as on cardiac function and mass (Caiani et al., 2014). Increasing the daily exposure to 60 min showed some interest regarding orthostatic tolerance, but did not prevent the reduction of plasma volume, stroke volume, and other indices of the cardiac function in another 21-day HDT bed rest study (Stenger et al., 2012).

It has already been reported that this intensity of artificial gravity can be well tolerated by the subjects: in this study, only 10 runs were prematurely stopped due to pre-syncope symptoms, out of a total of 960 (Frett et al., 2020b). It can be hypothesized that a larger load factor and/or longer exposure time may be used without compromising the safety of the subjects. To this respect, Iwasaki and colleagues have shown that exposure to a daily load factor of 2 g (at the feet) for 1 h could prevent changes in resting *HR*, sympathovagal balance, arterial cardiac baroreflex gains, and hematocrit caused by 4 days of HDT bed rest (Iwasaki et al., 2001). During another HDT bed rest study of a similar duration, a passive exposure to 1 g (standing position) during 2 h per day partially prevented decreases in orthostatic tolerance, and completely prevented it when the exposure was extended to 4 h per day (Vernikos et al., 1996). Finally, several animal studies have shown that daily exposure to 1 g (obtained by standing) could prevent vascular

remodeling (Sun et al., 2004; Gao et al., 2012) as well as myocardial contractility depression (Zhang et al., 2003).

However, artificial gravity alone simply reproduces the effect of standing in a gravity environment, which is not very demanding for the cardiorespiratory system. Thus, this countermeasure is not effective in maintaining aerobic exercise capacity and does not completely protect against the deterioration of muscle function (Kramer et al., 2021). The subjects remain hypokinetic and, in the absence of regular and significant increases in the cardiorespiratory demand (e.g., *via* physical exercises), associated with increases in blood flow and WSS, it is reasonable to expect a similar deconditioning as the one observed in sedentary individuals. Since many countermeasures based on physical exercise have already shown their efficacy to counteract (simulated) microgravity-induced cardiovascular deconditioning (Greaves et al., 2019; Rabineau et al., 2020), another interesting alternative could be to combine artificial gravity and physical exercise (Yang et al., 2010). Indeed, the added value of active *versus* passive exposure to 1 g (controlled walking *versus* standing) regarding the preservation of peak oxygen uptake during a 4-day HDT bed rest study has been demonstrated (Vernikos et al., 1996). In various additional HDT studies from 4 to 14 days, the combination of ergometric exercise with artificial gravity was also effective in preserving plasma volume (Iwase, 2005), stroke volume (Yang et al., 2011), autonomic function (Wang et al., 2011), and orthostatic tolerance (Li et al., 2017). However, even though it has been shown that repetitive jumping exercises were tolerated during short-arm centrifugation (Frett et al., 2020a), involuntary head movements may lead to motion sickness (Young et al., 2001; Iwase, 2005).

An interesting alternative to provide a fluid redistribution towards the lower body, as in a gravity environment, is the use of lower-body negative pressure (LBNP). Indeed, as opposed to the centrifuge, it does not put the subject in a rotating environment. Besides this, it is much smaller and less demanding in terms of power, technical expertise, etc. In addition to increasing LBNP tolerance (Watenpaugh et al., 1994), the combination of LBNP and physical exercise was proven to be more effective than LBNP alone in improving the orthostatic tolerance among ambulatory subjects, especially among females (Evans et al., 2018). During HDT bed rest, combined LBNP and exercise countermeasures have been effective in preserving blood volume (Guinet et al., 2009) and aerobic capacity (Hargens and Richardson, 2009). Watenpaugh and colleagues also showed the interest of adding a short rest period at the end of exercise, while continuing LBNP (Watenpaugh et al., 2007). Indeed, orthostatic stimulation immediately after exercise provides a greater cardiovascular stress than it does prior to exercise. This can be due to many factors including the ongoing skeletal muscle and cutaneous vasodilation, the reduction in vasoconstrictive sympathetic nerve activity, and the cessation of skeletal muscle pumping (Watenpaugh et al., 2007). Still, LBNP does not apply the exact

same pressure gradient in the circulation as gravity, including at the level of the cerebral circulation, carotid, and aortic baroreceptors. It is also unable to stimulate the vestibular system, which impacts vestibulo-vascular control mechanisms (Watenpaugh et al., 2007).

## Changes in blood flow

During the HDT phase, the observed increase in *HR* and decrease in  $SV_{tot}$  and  $CO_{tot}$  are in agreement with other investigations conducted during the same study (Kramer et al., 2020; Hoffmann et al., 2021; Möstl et al., 2021). Similar results have also been found in other HDT bed rest studies of various durations (Zhang et al., 1997; Spaak et al., 2005; Caiani et al., 2018; Maggioni et al., 2018; Rabineau et al., 2020). These changes are caused, among others, by the reduced cardiac preload, induced by a reduced volume of circulating blood (Watenpaugh and Hargens, 2011). In addition, the fact that parameters such as  $SV_{tot}$  continued to decrease between HDT5 and HDT56 could be explained by ventricular remodeling (Perhonen et al., 2001). The same observations were derived from animal models with, among others, hypovolemia, resting tachycardia, and decreased tolerance to lower-body negative pressure (Zhang, 2013). The cardiac mass of rats was not affected by 4 weeks of hindlimb unloading (Ray et al., 2001), whereas such conditions led to a decrease in the systolic function, as expressed by the maximum of  $dP/dt$ , possibly due to an impaired  $Ca^{2+}$  homeostasis (Cui et al., 2010). 2 weeks of exposure to microgravity has also been shown to lead to a decrease in papillary muscle myofiber area (Goldstein et al., 1992).

The blood supply is not similarly affected in the upper and lower body, as reflected by the increase of  $\%CO_{up}$  in Table 2, expressing a larger relative decrease in  $SV_{low}$  than in  $SV_{up}$ , which is also observed for  $Q_{max,DA}$  *versus*  $Q_{max,AA}$ . These observations seem to suggest that the oxygen supply to the brain is relatively preserved during HDT bed rest, while a potential decrease of  $CO_{up}$  could also be compensated by the increased hematocrit generally observed in such studies (Linnarsson et al., 2015; Palombo et al., 2015). However, another study has reported a decrease in cerebral blood flow after 26.5 h in  $-12^\circ$  HDT position (Kramer et al., 2017), suggesting that the underlying mechanisms may take some time to be fully applied. After 1 month in space, the ratio of carotid and femoral flows has been shown to increase (Herault et al., 2000), while it did not change after 4 days of dry immersion (Greaves et al., 2021), another analogue of microgravity. Previous HDT bed rest studies have already found similar results related to the non-uniform evolution of blood flow parameters in the upper *versus* lower body (Yuan et al., 2015; Caiani et al., 2016; Navasolava et al., 2020). Similar observations were also made in rats during hindlimb unloading (Colleran et al., 2000). This is an expected result, when the

subjects are observed in HDT *versus* horizontal supine position, because of the induced blood shift and its consequences. However, in this study, all the measurements were conducted in horizontal position, suggesting the influence of other parameters. This is also supported by the fact that % $CO_{up}$  was still higher than baseline at R+4.

Even though it was not found in a recent spaceflight study (Lee et al., 2020), the increase of SVR is also a common result of HDT bed rest studies (Zhang et al., 1997; Navasiolava et al., 2020). However, these changes in vascular resistance may be different between the upper and the lower body and thus explain the differences observed in terms of blood flow. Indeed, while an increase in vascular resistance is often observed in the lower limbs (Kamiya et al., 2000; Pawelczyk et al., 2001), it is usually not the case for the upper limbs (Zhang et al., 1997; Yang et al., 2011; Navasiolava et al., 2020). Several authors observed no changes in the main carotid artery blood velocity following exposure to HDT bed rest (Traon et al., 1995; Zhang et al., 1997), while others observed a decreased cerebral blood flow (Sun et al., 2005) that may be caused by an increased cerebral venous pressure (Yang et al., 2011). More generally, many authors reported vascular alterations in the lower body, while vessels of the upper body were left relatively unaffected (Platts et al., 2009; Palombo et al., 2015; Yuan et al., 2015).

## Evolution of arterial stiffness

$TAC$  has been shown to decrease with age, as well as hypertension, diabetes mellitus, and atherosclerosis (Haluska et al., 2008). Here, the observed decrease in  $TAC$  during the HDT phase is in agreement with data published by Lee and colleagues on long-duration (>4 months) spaceflights (Lee et al., 2020), even though they did not observe an overshoot following return to the Earth. In another study, Hoffmann and colleagues tested cosmonauts before and after a long-duration flight, and reported a decreased normalized systolic pressure amplification, suggesting an increased compliance of the arterial vasculature post- *versus* pre-flight (Hoffmann et al., 2019). The compliance of the proximal aorta decreased in rats after exposure to 7 days of hindlimb unweighting (Tuday et al., 2007), another analogue of microgravity. A decrease in femoral compliance was also observed after 60 days of HDT bed rest (Yuan et al., 2015), while no significant changes in carotid and brachial artery distensibility were observed after spaceflight (Lee et al., 2020). Interestingly,  $TAC$  did not change among the very same subjects as in this study, when it was computed based on an estimation of the aortic pulse pressure and measuring SV in HDT position using ultrasound (instead of MRI in horizontal position, as in this paper) (Möstl et al., 2021). Here, the decrease in  $TAC$  is mathematically caused by the decrease in  $SV_{tot}$ , while the pulse pressure remained relatively stable. Nevertheless, it is not possible to directly conclude that the decrease of  $TAC$  is

the consequence of an increase in the stiffness of the central arteries. Indeed, by definition,  $TAC$  is a global parameter that is a function of central and peripheral arterial stiffness and that can be influenced by many other elements of the circulatory system, including peripheral vasoconstriction.

In contrast,  $PWV$ ,  $CAVI$ , and  $CAVI_0$  represent the local stiffness of the aorta. This is a very interesting element of this study as, in most clinical trials, these three parameters are measured based on the carotid-femoral  $PWV$ , thus also including thinner and stiffer vessels (carotid, iliac, and femoral arteries). Other things being equal, a greater  $PWV$  indicates stiffer arteries, but there are many confounding factors, including blood pressure (Spronck et al., 2017). Here, we indeed report an increase of  $DBP$  and  $SBP$ , while other investigations with the same subjects described an increase in the cross-section area of the aorta (ref Mostl et al., 2021). It has been shown that changes of 10 mmHg in the diastolic blood pressure could lead to a difference of 1 m/s in  $PWV$  (Spronck et al., 2015). However, this relationship is relatively complex and age-specific (Spronck et al., 2015). To address this interaction issue, Shirai and colleagues introduced the  $CAVI$  parameter (Shirai et al., 2006), which, even though named “cardio-ankle”, can be applied to any  $PWV$  measurement. An updated version ( $CAVI_0$ ) has also recently been suggested (Spronck et al., 2017). However, both  $CAVI$  and  $CAVI_0$  are highly correlated among healthy subjects (Lin et al., 2020) and it is still not clear which of these two is the best one (Takahashi et al., 2020; Giudici et al., 2021). Still, even using these parameters adjusted for blood pressure, the results in the HDT phase indicate stiffer aortas. The fact that these three markers of aortic stiffness were back to their initial values following only 4 days of recovery, indicates functional rather than structural changes.

The observed changes in these markers of stiffness could be hypothesized to be at least partially due to a decrease in left ventricular ejection time (LVET). Indeed, *in silico* and clinical results have shown that there is an inverse relationship between LVET and  $PWV$  (Salvi et al., 2013; Lillie et al., 2015). Besides this,  $DBP$  and LVET are independent predictors of  $PWV$  (Nürnbergberger et al., 2003). Published results based on the same study, with the same subjects, have shown a decrease of approximately 30 ms in LVET (Orter et al., 2022), in agreement with other HDT bed rest studies (Caiani et al., 2018; Hoffmann et al., 2022). However, it has been shown that a decrease of ~40 ms in LVET could lead to an increase of ~1 m/s in  $PWV$  (Nürnbergberger et al., 2003), which is close to what is observed here. Moreover, LVET has been shown to quickly return to baseline values after HDT bed rest (Caiani et al., 2018; Orter et al., 2022), which is also what is found here regarding  $PWV$ .

The median increase in  $PWV$  at the end of the HDT phase was 0.9 m/s, which corresponds to about a decade of transient vascular aging (The Reference Values for Arterial Stiffness' Collaboration, 2010; Harloff et al., 2018). The commonly

accepted threshold over which *PWV* is considered to represent an increased cardiovascular risk is 10 m/s (Williams et al., 2018). While all the subjects were below this limit at BDC-9, one of them exceeded it at HDT21 and HDT56. It may be worth noting that this subject was also the oldest one (54 years old). The median increases in *CAVI* and *CAVI<sub>0</sub>* at HDT56 also correspond to more than a decade of healthy vascular aging (Shirai et al., 2019). According to the Japan Society for Vascular Failure, *CAVI* is considered abnormal when it reaches values greater than 9 (Tanaka et al., 2017). Applying this criterion in this study, 6 subjects had abnormally high values of *CAVI* at HDT56, even though it was already the case for 2 of them at BDC-9. Overall, these observations agree with recent spaceflight studies suggesting 10–20 years of vascular aging following exposure to microgravity (Arbeille et al., 2016; Hughson et al., 2016).

Hoffmann and colleagues reported no changes in *PWV* after long-duration spaceflights (Hoffmann et al., 2019), while other teams observed a decreased pulse wave arrival time at the finger on return to Earth, after 1–2 days (Hughson et al., 2016) and after 3–6 days (Baevsky et al., 2007). In addition, it was shown that this pulse arrival time was also decreased compared to baseline during the actual spaceflight (Baevsky et al., 2007). In a study conducted with rats, 7 days of hindlimb unweighting were sufficient to observe a large increase of *PWV* in the thoracic aorta, but no changes in the abdominal aorta (Tuday et al., 2007). In contrast, no changes were reported in carotid-femoral and carotid to tibial *PWV* following 4 days of dry immersion in humans (Greaves et al., 2021). Results in other HDT bed rest studies are not clear and, while carotid-femoral *PWV* was left unchanged following 35 days in HDT position (Palombo et al., 2015), others have found an increase of more than 1 m/s after 60 days of HDT bed rest, with no return to baseline values 1 year after the study (Fayol et al., 2019). A recent study also found a decrease of pulse transit time to the finger following exposure to HDT bed rest (Hoffmann et al., 2022). Interestingly, no changes in brachial-femoral *PWV* were observed within the same participants as the ones of this paper (Möstl et al., 2021). These different findings might be explained by a different methodology, in particular the position that was chosen during the HDT phase to evaluate the parameters of interest: horizontal here, versus HDT in Möstl's paper. In addition, brachial-femoral *PWV* includes stiffer vessels, as can be seen by its average value: 9.0 versus 5.3 when comparing baseline values. Thus, the evolutions of aortic and brachial-femoral *PWV* certainly reflect different types of adaptations.

## Changes in wall shear stress

In this study, the observed decrease in the amplitude of aortic *WSS* is certainly the direct consequence of the decrease in both mean and peak flow in the aorta. Despite this decrease, *WSS<sub>mean</sub>* and *TAWSS* remained in the range of normal values for healthy

subjects, while *OSI* was markedly smaller than average in this cohort all along the study (Callaghan and Grieve, 2018; van der Palen et al., 2018; Trenti et al., 2022). In addition to the resting *WSS*, HDT bed rest studies also prevent regular increases in *WSS* caused by physical exercise, since lower limbs are underused. Indeed, it has been shown that lower limb exercise caused large increases in *TAWSS* and large decreases in *OSI* in the abdominal aorta (Tang et al., 2006).

After 5 weeks of HDT bed rest, Palombo and colleagues did not observe such a decrease in peak wall shear rate in the common carotid and femoral arteries, but they also did not report any changes in mean and systolic flows through these arteries (Palombo et al., 2015). Incidentally, what is reported as *WSS* in the present paper in fact reflects more the evolution of wall shear rate, since the blood viscosity was considered constant. The literature is not very conclusive regarding the exact evolution of blood viscosity in (simulated) weightlessness and experiments in animal models have found either an increase (Shen et al., 1997; Li et al., 2002; Saunders et al., 2002) or no changes (Ryou, 2003; Hu et al., 2017). Remaining in sitting position during 2 hours has also been shown to increase blood viscosity (Hitosugi et al., 2000). Thus, the reported results may overestimate the actual decrease of *WSS<sub>mean</sub>* and *TAWSS*.

When the amplitude of *WSS* decreases and/or when it becomes more multidirectional, the vascular endothelial cells detect these changes, decrease the release of nitric oxide (NO), and induce the atherogenic processes of the aortic wall (Thijssen et al., 2011a). Computational fluid dynamics model have shown that high *WSS* magnitude in coronary arteries protected against atherosclerosis (Mahmoudi et al., 2020), while low *WSS* magnitude led to vascular remodeling and thickening of the vascular wall (Chen et al., 2022). More generally, the magnitude of *WSS* was found to be inversely correlated with intima-media thickness (Irace et al., 2004).

One could thus argue that the decrease in *WSS<sub>mean</sub>* and *TAWSS* is the reason behind the increased carotid and femoral intima-media thickness found in spaceflight (Arbeille et al., 2016). In HDT bed rest, these changes are not systematically reported (Palombo et al., 2015; Yuan et al., 2015), but van Duijnhoven and colleagues noticed them, and observed that a countermeasure based on physical exercise could even reduce them (van Duijnhoven et al., 2010). In rabbits with a high-fat diet meant to cause atherosclerosis, a decrease in the magnitude of *WSS* was observed already 4 weeks before an increase in intima-media thickness (Zhang et al., 2017). However, in the case of spaceflight, the femoral intima-media thickness was back to baseline values after only 4 days (Arbeille et al., 2016), which seems against the hypothesis of atherosclerotic-based changes. On the contrary, the main reason behind these short-term changes in arterial wall thickness may originate from reversible physiological adaptations, potentially at the level of the smooth muscle cells in the media layer (Thijssen et al., 2011a). This hypothesis is supported by the fact that

pharmacological smooth muscle relaxation has been shown to lead to large (10%) and immediate (less than 10 min) reductions in carotid and femoral artery wall thickness (Thijssen et al., 2011b).

An increased vasomotor sympathetic nerve activity and decreased plasma NO has been shown following HDT bed rest (Kamiya et al., 2000). This decreased NO bioavailability increases the vascular tone and promotes the proliferation of smooth muscle cells (Atochin and Huang, 2010). It is thus possible that the observed increase in *RRT* is the consequence of vascular wall thickening. Indeed, Chen and colleagues have shown the correspondence between the regions of vascular remodeling and those of high *RRT* (Chen et al., 2017). Other studies also suggested that the areas of high *RRT* may predict plaque initiation and growth rate (Soulis et al., 2011; Rikhtegar et al., 2012; Hoogendoorn et al., 2020).

In an *ex vivo* experiment, the smooth muscle activation was shown to lead to an increase in aortic stiffness (Franchini et al., 2022). It seems in line with spaceflight findings, where a positive relationship has been observed between carotid intima-media thickness and  $\beta$ -stiffness (Arbeille et al., 2016). This may be the actual reason why an increase in all the markers of aortic stiffness was found during the HDT phase, with such a quick return to baseline values during recovery. However, it has to be expected that the amplitude of changes and the time of recovery may not be the same in conduit vessels like the aorta and in resistance vessels. Still, experiments conducted on hindlimb unloaded rats have shown that the differential regulation of intracellular  $\text{Ca}^{2+}$  in cerebral and small mesenteric arterial smooth muscle cells was no longer visible after only 3 days of recovery (Xue et al., 2011).

## Differences between male and female subjects

Up to now, female astronauts represent only a small share of the overall population that has flown to space. The same holds true for the participants to studies in the field of altered gravity, including HDT bed rest studies. Only in the recent years, space agencies have tried to reduce this gap by enrolling more female volunteers in such studies, which is even more important as males and females are known to be affected differently by exposure to microgravity (Platts et al., 2014).

In particular, female astronauts are more susceptible to orthostatic intolerance than their male counterparts, with difficulties in maintaining venous return and cardiac output in the upright posture (Harm et al., 2001). Among other factors, this could be due to the indirect vasodilatory effects of estrogen, leading to a smaller vasoconstrictive responsiveness among women (Fritsch-Yelle et al., 1996). In addition, female astronauts experience a larger decrease in plasma volume

following spaceflight (Waters et al., 2002), while HDT bed rest studies have come to contradictory findings regarding this parameter (Platts et al., 2014).

Some gender-dependent changes in arterial stiffness may also explain the differences observed in terms of orthostatic tolerance (Tuday et al., 2011). After 6 months in space, it was found that the  $\beta$ -stiffness index in the carotid artery increased more in women than in men, while the opposite was found for the pulse transit time to the finger and to the posterior tibial artery (Hughson et al., 2016). It was also shown, both in HDT bed rest and spaceflight, that arterial stiffness expressed as the inverse of *TAC* was stable among females, while it increased for males (Tuday et al., 2011). Interestingly, in this study, no gender difference has been found regarding the evolution of *TAC*. The same holds true for the markers of aortic stiffness such as *PWV*, *CAVI*, and *CAVI<sub>0</sub>* (Table 3). However, the gender-differences found in *TAWSS* and *RRT* (Figure 4) seem to indicate a context that is potentially more prone to vascular remodeling (Thijssen et al., 2011a; Chen et al., 2017) in males than in females, for which these parameters are left relatively unchanged.

Cardiac atrophy, as well as the related impact of exercise, has been shown to occur similarly in males and females during HDT bed rest (Dorfman et al., 2007; Platts et al., 2014; Evans et al., 2018). In addition, no gender differences were observed for stroke volume and cardiac output indices following spaceflight (Waters et al., 2002). This is in line with the absence of a significant effect of sex  $\times$  time observed here on *SV<sub>tot</sub>* and *CO<sub>tot</sub>*.

During a 28-day HDT bed rest study, a protocol combining LBNP and exercise was shown to be able to reduce orthostatic tolerance, without reporting differences between men and women (Watenpaugh et al., 2007). In another study with ambulatory subjects, 3 weeks of passive artificial gravity training improved orthostatic tolerance in males but not in females (Stenger et al., 2007). Here, no sex  $\times$  group and no sex  $\times$  group  $\times$  time differences were observed for any of the parameters studied.

Due to the very low number of females included in each group, the relevant statistical power may not have been sufficient to provide a clear conclusion regarding the absence of gender-related differences in the different markers, including the distribution of blood flow and aortic stiffness. Accordingly, we encourage future HDT bed rest studies to enroll more women to be able to answer such questions.

## Limitations

As most of the HDT bed rest studies, this research is limited by the number of included subjects. In particular, the distribution in three different groups of 8 subjects may have hidden a potential small effect of the applied countermeasure. While, it

has been recommended to evaluate gender differences related to artificial gravity countermeasures (Evans et al., 2018), here there were only 2 to 3 women in each group. Even if no gender  $\times$  group (results not presented) and only a few gender  $\times$  time differences were observed, it is not possible to come with a clear conclusion regarding gender differences, given the very low number of female subjects in each group.

In such studies involving many experiments and paired groups, it is very difficult to control the timing of a specific protocol with regard to the menstrual cycle phase. Even HDT bed rest studies including only women often lack this type of control (Guinet et al., 2009). However, differences in the balance of ovarian hormones during the menstrual cycle have an impact on autonomic functions (Dimitriev et al., 2007), which can impact orthostatic tolerance. In addition, the menstrual cycle has been reported to have an impact on resting heart rate (Moran et al., 2000), on systolic and diastolic functions of both ventricles (Zengin et al., 2007), as well as on smooth muscle sensitivity to NO and whole-body arterial compliance (Williams et al., 2001), while central arterial stiffness remains relatively preserved (Ounis-Skali et al., 2006). We encourage including more women in future HDT bed rest studies so that the exact impact of this confounding factor can be better understood.

The 4D flow cardiac MRI acquisitions were all started after approximately 40 min in horizontal supine position, even during the HDT phase. On the one hand, this may not be representative of the actual cardiovascular state of the subjects at each step of the study, but on the other hand, it also helps to better compare the results at the different time points.

HDT bed rest results cannot readily be extended to actual microgravity as some dissimilarities remain. Indeed, the body is not in absolute weightlessness during HDT bed rest studies, which may have an impact on some cardiovascular parameters. For instance, Lee and colleagues argued that unweighting of the neck tissue overlying the common carotid artery may play a key role in space, allowing the vessel to expand, while gravity still acts upon the neck tissue in HDT bed rest and the diameter of the common carotid artery remains unchanged (Lee et al., 2020).

In addition, the fitness status of the participants was lower than the one of the astronaut population, especially when correcting for the age (Moore et al., 2014; Kramer et al., 2021). Indeed, at the time of their first flight, astronauts are usually older by about one decade than the participants of this study (Kovacs and Shadden, 2017). Thus, precautions should be taken when trying to extend these results to the whole astronaut population.

Several parameters were computed based on the brachial blood pressure, while the aortic blood pressure would have been more relevant, if it had been possible to measure it. This is particularly the case of  $CAVI$  and  $CAVI_0$ .

Finally, the 4D flow cardiac MRI protocol had a relatively low temporal resolution, especially for low heart rates, with only 20 images per cardiac cycle. It has been shown that this could lead

to an underestimation of peak flow rate (Dyverfeldt et al., 2015), but also of  $OSI$  (Cibis et al., 2016). However, this does not challenge our conclusions regarding blood flow and  $WSS$ , as we discussed relative differences. In addition, the chosen method for the evaluation of aortic  $PWV$  has been proven to lead to only negligible differences between an acquisition at 50 images per cardiac cycle, and a subset of this acquisition corresponding to 20 images per cardiac cycle (Houriez–Gombaudo–Saintonge et al., 2019).

We believe that these limitations did not preclude any of the conclusion of this research.

## Conclusion

We demonstrated the potential of 4D flow cardiac MRI to assess the longitudinal evolution of several cardiovascular parameters through a 60-day strict HDT bed rest study. To our knowledge, this is the first time that 4D flow cardiac MRI is used in this context, thus overcoming limitations of other imaging techniques, and enabling the evaluation of many aortic parameters that were never measured in simulated microgravity. In the absence of significant differences between the different groups studied, we can conclude that the effects of the applied artificial gravity countermeasures were either absent or too weak to reach statistical significance. Future evaluations of potential countermeasures based on artificial gravity should either increase the load factor, the time of exposure, or combine it with physical exercise. The observed changes in blood flow confirmed the different adaptations occurring in the upper and lower body during exposure to (simulated) microgravity. A larger share of blood volume was dedicated to the upper body during the HDT phase, which helps cerebral perfusion. All the markers of arterial stiffness indicated a more rigid aorta during the HDT phase, which may be caused by the decrease in the magnitude of  $WSS$  and/or by other hemodynamic changes including a decrease in  $LVET$ . Interestingly, some changes in  $WSS$  parameters were observed only in males during the HDT phase, while females experienced opposite changes during recovery. No other gender-related differences were observed but future studies should investigate these aspects in more detail by including more female subjects. All the changes in aortic stiffness and  $WSS$  parameters remained subclinical, as probably the sole consequence of functional—rather than structural—changes. Indeed, most of the modifications tended to or returned to baseline already after 4 days of recovery, thus indicating no permanent cardiovascular adaptations following 60 days of strict HDT bed rest. Still, these observations trigger the need to evaluate these parameters or their proxies during long duration space travels, including potential remote monitoring, to verify if changes remain subclinical or if they translate in clinical manifestation, thus posing the need to assess a potential risk evolution profile.

## Data availability statement

The raw data supporting the conclusion of this article will be made available by the authors, without undue reservation.

## Ethics statement

The studies involving human participants were reviewed and approved by the Northern Rhine Medical Association (Ärztammer Nordrhein, application N°2018143) and Federal Office for Radiation Protection (Bundesamt für Strahlenschutz, application N°22464/2018-074-R-G). The patients/participants provided their written informed consent to participate in this study.

## Author contributions

EC, JT, and P-FM designed the experiment. DG provided support for the 4D Flow cardiac MRI protocol. FH and JR performed data acquisition. JR and MI had full access to all the data of this study and take responsibility for the integrity of the data and the accuracy of data analysis. JR and MI performed the statistical analysis. JR drafted the manuscript. All the authors revised critically the manuscript and accepted the final version.

## Funding

The AGBRESA study was funded by DLR, ESA (contract number 4000113871/15/NL/PG), and NASA (contract number 80JSC018P0078). JR is supported by the Fonds de la Recherche Scientifique (Mandat Aspirant F.R.S.—FNRS FC 29801). FH

## References

- Arbeille, P., Provost, R., and Zuj, K. (2016). Carotid and femoral artery intima-media thickness during 6 Months of spaceflight. *Aerosp. Med. Hum. Perform.* 87, 449–453. doi:10.3357/AMHP.4493.2016
- Atochin, D. N., and Huang, P. L. (2010). Endothelial nitric oxide synthase transgenic models of endothelial dysfunction. *Pflugers Arch.* 460, 965–974. doi:10.1007/s00424-010-0867-4
- Baevsky, R. M., Baranov, V. M., Funtova, I. I., Diedrich, A., Pashenko, A. V., Chernikova, A. G., et al. (2007). Autonomic cardiovascular and respiratory control during prolonged spaceflights aboard the International Space Station. *J. Appl. Physiol.* 103, 156–161. doi:10.1152/jappphysiol.00137.2007
- Bargiotas, I., Mousseaux, E., Yu, W.-C., Venkatesh, B. A., Bollache, E., de Cesare, A., et al. (2015). Estimation of aortic pulse wave transit time in cardiovascular magnetic resonance using complex wavelet cross-spectrum analysis. *J. Cardiovasc. Magn. Reson.* 17, 65. doi:10.1186/s12968-015-0164-7
- Benjamini, Y., Krieger, A. M., and Yekutieli, D. (2006). Adaptive linear step-up procedures that control the false discovery rate. *Biometrika* 93, 491–507. doi:10.1093/biomet/93.3.491
- Blomqvist, C. G., and Stone, H. L. (1983). “Cardiovascular adjustments to gravitational stress,” in *Comprehensive Physiology*. Editor R. Terjung (New Jersey: Wiley), 1025–1063. doi:10.1002/cphy.cp020328
- Caiani, E. G., Landreani, F., Costantini, L., Mulder, E., Gerlach, D. A., Vaida, P., et al. (2018). Effectiveness of high-intensity jump training countermeasure on mitral and aortic flow after 58-days head-down bed-rest assessed by phase-contrast MRI Bremen, Germany). Available at: <https://elib.dlr.de/126169/> [Accessed May 6, 2022].
- Caiani, E. G., Massabuau, P., Weinert, L., Vaida, P., and Lang, R. M. (2014). Effects of 5 days of head-down bed rest, with and without short-arm centrifugation as countermeasure, on cardiac function in males (BR-AG1 study). *J. Appl. Physiol.* 117, 624–632. doi:10.1152/jappphysiol.00122.2014
- Caiani, E. G., Riso, G., Landreani, F., Martin-Yebra, A., Pirola, S., Piatti, F., et al. (2016). “Aortic flow and morphology adaptation to deconditioning after 21-days of head-down bed-rest assessed by phase contrast MRI,” in *Computing in Cardiology Conference (CinC)*, 2016 (IEEE), Vancouver, BC, Canada, 11–14 September 2016, 73. Available at: <http://ieeexplore.ieee.org/abstract/document/7868682/> (Accessed May 31, 2017).
- Callaghan, F., and Grieve, S. (2018). Normal patterns of thoracic aortic wall shear stress measured using four-dimensional flow MRI in a large population. *Am. J. Physiol. Heart Circ. Physiol.* 315, H1174–H1181. doi:10.1152/ajpheart.00017.2018
- Chen, S., Zhang, H., Hou, Q., Zhang, Y., and Qiao, A. (2022). Multiscale modeling of vascular remodeling induced by wall shear stress. *Front. Physiol.* 12, 808999. doi:10.3389/fphys.2021.808999

received funding by the DLR and the German Federal Ministry of Economy and Technology, BMWi (50WB1816). P-FM is supported by a grant from the European Space Agency and the Belgian Federal Scientific Policy Office (PRODEX PEA 4000110826). EC is supported by the Italian Space Agency (contracts 2018-7-U.0, 2022-9-U.0 and 2022-10-U.0).

## Acknowledgments

We would like to thank the entire team at the DLR, including Edwin Mulder and Jessica Lee for the management of the whole study, as well as Kerstin Kempter and Annette von Waechter for generating the cardiac MRI data. We would also like to thank the 24 subjects of the AGBRESA study for their cooperation.

## Conflict of interest

The authors declare that the research was conducted in the absence of any commercial or financial relationships that could be construed as a potential conflict of interest.

## Publisher's note

All claims expressed in this article are solely those of the authors and do not necessarily represent those of their affiliated organizations, or those of the publisher, the editors and the reviewers. Any product that may be evaluated in this article, or claim that may be made by its manufacturer, is not guaranteed or endorsed by the publisher.

- Chen, Z., Yu, H., Shi, Y., Zhu, M., Wang, Y., Hu, X., et al. (2017). Vascular remodelling relates to an elevated oscillatory shear index and relative residence time in spontaneously hypertensive rats. *Sci. Rep.* 7, 2007. doi:10.1038/s41598-017-01906-x
- Cibis, M., Potters, W. V., Gijsen, F. J., Marquering, H., Ooij, P., vanBavel, E., et al. (2016). The effect of spatial and temporal resolution of cine phase contrast MRI on wall shear stress and oscillatory shear index assessment. *PLOS ONE* 11, e0163316. doi:10.1371/journal.pone.0163316
- Colleran, P. N., Wilkerson, M. K., Bloomfield, S. A., Suva, L. J., Turner, R. T., and Delp, M. D. (2000). Alterations in skeletal perfusion with simulated microgravity: a possible mechanism for bone remodeling. *J. Appl. Physiol.* 89, 1046–1054. doi:10.1152/jappl.2000.89.3.1046
- Cui, Y., Zhang, S.-M., Zhang, Q.-Y., Fan, R., Li, J., Guo, H.-T., et al. (2010). Modulation of intracellular calcium transient in response to beta-adrenoceptor stimulation in the hearts of 4-wk-old rats during simulated weightlessness. *J. Appl. Physiol. Md* 1985 108, 838–844. doi:10.1152/jappphysiol.01055.2009
- Delp, M. D. (2007). Arterial adaptations in microgravity contribute to orthostatic tolerance. *J. Appl. Physiol.* 102, 836. doi:10.1152/jappphysiol.01347.2006
- Demir, A., Wiesemann, S., Erley, J., Schmitter, S., Trauzeddel, R. F., Pieske, B., et al. (2022). Traveling volunteers: A multi-vendor, multi-center study on reproducibility and comparability of 4D flow derived aortic hemodynamics in cardiovascular magnetic resonance. *J. Magn. Reson. Imaging* 55, 211–222. doi:10.1002/jmri.27804
- Dimitriev, D. A., Saperova, E. V., Dimitriev, A. D., and Karpenko, I. D. (2007). Features of cardiovascular functioning during different phases of the menstrual cycle. *Russ. Fiziol. Zh. Im. I. M. Sechenova* 93, 300–305.
- Dorfman, T. A., Levine, B. D., Tillery, T., Peshock, R. M., Hastings, J. L., Schneider, S. M., et al. (2007). Cardiac atrophy in women following bed rest. *J. Appl. Physiol.* 103, 8–16. doi:10.1152/jappphysiol.01162.2006
- Dyverfeldt, P., Bissell, M., Barker, A. J., Bolger, A. F., Carlhäll, C.-J., Ebbens, T., et al. (2015). 4D flow cardiovascular magnetic resonance consensus statement. *J. Cardiovasc. Magn. Reson.* 17, 72. doi:10.1186/s12968-015-0174-5
- Evans, J. M., Knapp, C. F., and Goswami, N. (2018). Artificial gravity as a countermeasure to the cardiovascular deconditioning of spaceflight: Gender perspectives. *Front. Physiol.* 9, 716. doi:10.3389/fphys.2018.00716
- Fayol, A., Mallois-Delaunay, J., Fouassier, D., Cristian, C., Leguy, C., Bareille, M. P., et al. (2019). Impact of 60 Day of bedrest on long-term pulse wave velocity evolution. *J. Hypertens. Los. Angel.* 37, e85. doi:10.1097/01.hjh.0000570256.58051.21
- Franchini, G., Breslavsky, I. D., Giovannello, F., Kassab, A., Holzapfel, G. A., and Amabili, M. (2022). Role of smooth muscle activation in the static and dynamic mechanical characterization of human aortas. *Proc. Natl. Acad. Sci. U. S. A.* 119, e2117232119. doi:10.1073/pnas.2117232119
- Frett, T., Green, D. A., Arz, M., Noppe, A., Petrat, G., Kramer, A., et al. (2020a). Motion sickness symptoms during jumping exercise on a short-arm centrifuge. *PLOS ONE* 15, e0234361. doi:10.1371/journal.pone.0234361
- Frett, T., Green, D. A., Mulder, E., Noppe, A., Arz, M., Pustowalow, W., et al. (2020b). Tolerability of daily intermittent or continuous short-arm centrifugation during 60-day 60 head down bed rest (AGBRESA study). *PLOS ONE* 15, e0239228. doi:10.1371/journal.pone.0239228
- Fritsch-Yelle, J. M., Whitson, P. A., Bondar, R. L., and Brown, T. E. (1996). Subnormal norepinephrine release relates to presyncope in astronauts after spaceflight. *J. Appl. Physiol.* 81, 2134–2141. doi:10.1152/jappl.1996.81.5.2134
- Gao, F., Cheng, J.-H., Bai, Y.-G., Boscolo, M., Huang, X.-F., Zhang, X., et al. (2012). Mechanical properties and composition of mesenteric small arteries of simulated microgravity rats with and without daily -G(x) gravitation. *Sheng Li Xue Bao* 64, 107–120.
- Giudici, A., Khir, A. W., Reesink, K. D., Delhaas, T., and Spronck, B. (2021). Five years of cardio-ankle vascular index (CAVI) and CAVIO: how close are we to a pressure-independent index of arterial stiffness? *J. Hypertens.* 39, 2128–2138. doi:10.1097/HJH.0000000000002928
- Goldstein, M. A., Edwards, R. J., and Schroeter, J. P. (1992). Cardiac morphology after conditions of microgravity during COSMOS 2044. *J. Appl. Physiol.* 73, 94S. doi:10.1152/jappl.1992.73.2.S94
- Greaves, D., Arbeille, P., Guillon, L., Zuj, K., and Caiani, E. G. (2019). Effects of exercise countermeasure on myocardial contractility measured by 4D speckle tracking during a 21-day head-down bed rest. *Eur. J. Appl. Physiol.* 119, 2477–2486. doi:10.1007/s00421-019-04228-0
- Greaves, D., Guillon, L., Besnard, S., Navasiolava, N., and Arbeille, P. (2021). 4 Day in dry immersion reproduces partially the aging effect on the arteries as observed during 6 month spaceflight or confinement. *Npj Microgravity* 7, 43–47. doi:10.1038/s41526-021-00172-6
- Guinet, P., Schneider, S. M., Macias, B. R., Watenpaugh, D. E., Hughson, R. L., Le Traon, A. P., et al. (2009). WISE-2005: effect of aerobic and resistive exercises on orthostatic tolerance during 60 days bed rest in women. *Eur. J. Appl. Physiol.* 106, 217–227. doi:10.1007/s00421-009-1009-6
- Haluska, B. A., Jeffriess, L., Downey, M., Carlier, S. G., and Marwick, T. H. (2008). Influence of cardiovascular risk factors on total arterial compliance. *J. Am. Soc. Echocardiogr.* 21, 123–128. doi:10.1016/j.echo.2007.05.043
- Hargens, A. R., Bhattacharya, R., and Schneider, S. M. (2013). Space physiology VI: exercise, artificial gravity, and countermeasure development for prolonged space flight. *Eur. J. Appl. Physiol.* 113, 2183–2192. doi:10.1007/s00421-012-2523-5
- Hargens, A. R., and Richardson, S. (2009). Cardiovascular adaptations, fluid shifts, and countermeasures related to space flight. *Respir. Physiol. Neurobiol.* 169, S30–S33. doi:10.1016/j.resp.2009.07.005
- Harloff, A., Mirzaee, H., Lodemann, T., Hagenlocher, P., Wehrum, T., Stuplich, J., et al. (2018). Determination of aortic stiffness using 4D flow cardiovascular magnetic resonance - a population-based study. *J. Cardiovasc. Magn. Reson.* 20, 43. doi:10.1186/s12968-018-0461-z
- Harm, D. L., Jennings, R. T., Meck, J. V., Powell, M. R., Putcha, L., Sams, C. P., et al. (2001). Invited review: Gender issues related to spaceflight: a NASA perspective. *J. Appl. Physiol.* 91, 2374–2383. doi:10.1152/jappl.2001.91.5.2374
- Herauld, S., Fomina, G., Alferova, I., Kotovskaya, A., Poliakov, V., and Arbeille, P. (2000). Cardiac, arterial and venous adaptation to weightlessness during 6-month MIR spaceflights with and without thigh cuffs (bracelets). *Eur. J. Appl. Physiol.* 81, 384–390. doi:10.1007/s004210050058
- Hitosugi, M., Niwa, M., and Takatsu, A. (2000). Rheologic changes in venous blood during prolonged sitting. *Thromb. Res.* 100, 409–412. doi:10.1016/S0049-3848(00)00348-0
- Hoffmann, B., Dehkordi, P., Khosrow-Khavar, F., Goswami, N., Blaber, A. P., and Tavakolian, K. (2022). Mechanical deconditioning of the heart due to long-term bed rest as observed on seismocardiogram morphology. *Npj Microgravity* 8, 25. doi:10.1038/s41526-022-00206-7
- Hoffmann, F., Möstl, S., Luchitskaya, E., Funtova, I., Jordan, J., Baevsky, R., et al. (2019). An oscillometric approach in assessing early vascular ageing biomarkers following long-term space flights. *Int. J. Cardiol. Hypertens.* 2, 100013. doi:10.1016/j.ijch.2019.100013
- Hoffmann, F., Rabineau, J., Mehrkens, D., Gerlach, D. A., Moestl, S., Johannes, B. W., et al. (2021). Cardiac adaptations to 60 day head-down-tilt bed rest deconditioning. Findings from the AGBRESA study. *Esc. Heart Fail.* 8, 729–744. doi:10.1002/ehf2.13103
- Hoogendoorn, A., Kok, A. M., Hartman, E. M. J., de Nisco, G., Casadonte, L., Chiastra, C., et al. (2020). Multidirectional wall shear stress promotes advanced coronary plaque development: comparing five shear stress metrics. *Cardiovasc. Res.* 116, 1136–1146. doi:10.1093/cvr/cvz212
- Houriez-Gombaudo-Saintonge, S., Mousseaux, E., Bargiotas, I., De Cesare, A., Diertenbeck, T., Bouaou, K., et al. (2019). Comparison of different methods for the estimation of aortic pulse wave velocity from 4D flow cardiovascular magnetic resonance. *J. Cardiovasc. Magn. Reson.* 21, 75. doi:10.1186/s12968-019-0584-x
- Hu, H.-X., Du, F.-Y., Fu, W.-W., Jiang, S.-F., Cao, J., Xu, S.-H., et al. (2017). A dramatic blood plasticity in hibernating and 14-day hindlimb unloading Daurian ground squirrels (*Spermophilus dauricus*). *J. Comp. Physiol. B* 187, 869–879. doi:10.1007/s00360-017-1092-7
- Hughson, R. L., Robertson, A. D., Arbeille, P., Shoemaker, J. K., Rush, J. W. E., Fraser, K. S., et al. (2016). Increased postflight carotid artery stiffness and in-flight insulin resistance resulting from 6-mo spaceflight in male and female astronauts. *Am. J. Physiol. Heart Circ. Physiol.* 310, H628–H638. doi:10.1152/ajpheart.00802.2015
- Hurst, C., Scott, J. P. R., Weston, K. L., and Weston, M. (2019). High-intensity interval training: A potential exercise countermeasure during human spaceflight. *Front. Physiol.* 10, 581. doi:10.3389/fphys.2019.00581
- Irace, C., Cortese, C., Fiaschi, E., Carallo, C., Farinano, E., and Gnasso, A. (2004). Wall shear stress is associated with intima-media thickness and carotid atherosclerosis in subjects at low coronary heart disease risk. *Stroke* 35, 464–468. doi:10.1161/01.STR.0000111597.34179.47
- Iwasaki, K., Sasaki, T., Hirayanagi, K., and Yajima, K. (2001). Usefulness of daily +2G load as a countermeasure against physiological problems during weightlessness. *Acta Astronaut.* 49, 227–235. doi:10.1016/S0094-5765(01)00101-1
- Iwase, S. (2005). Effectiveness of centrifuge-induced artificial gravity with ergometric exercise as a countermeasure during simulated microgravity exposure in humans. *Acta Astronaut.* 57, 75–80. doi:10.1016/j.actaastro.2005.03.013
- Kamiya, A., Iwase, S., Michikami, D., Fu, Q., Mano, T., Kitaichi, K., et al. (2000). Increased vasomotor sympathetic nerve activity and decreased plasma nitric oxide release after head-down bed rest in humans: disappearance of correlation between

- vasoconstrictor and vasodilator. *Neurosci. Lett.* 281, 21–24. doi:10.1016/S0304-3940(00)00804-1
- Kovacs, G. T. A., and Shadden, M. (2017). Analysis of age as a factor in NASA astronaut selection and career landmarks. *PLoS ONE* 12, e0181381. doi:10.1371/journal.pone.0181381
- Kramer, A., Venegas-Carro, M., Mulder, E., Lee, J. K., Moreno-Villanueva, M., Bürkle, A., et al. (2020). Cardiorespiratory and neuromuscular demand of daily centrifugation: Results from the 60-day AGBRESA bed rest study. *Front. Physiol.* 11, 562377. doi:10.3389/fphys.2020.562377
- Kramer, A., Venegas-Carro, M., Zange, J., Sies, W., Maffioletti, N. A., Gruber, M., et al. (2021). Daily 30-min exposure to artificial gravity during 60 days of bed rest does not maintain aerobic exercise capacity but mitigates some deteriorations of muscle function: results from the AGBRESA RCT. *Eur. J. Appl. Physiol.* 121, 2015–2026. doi:10.1007/s00421-021-04673-w
- Kramer, L. A., Hasan, K. M., Sargsyan, A. E., Marshall-Goebel, K., Rittweger, J., Donoviel, D., et al. (2017). Quantitative MRI volumetry, diffusivity, cerebrovascular flow, and cranial hydrodynamics during head-down tilt and hypercapnia: the SPACECOT study. *J. Appl. Physiol.* 122, 1155–1166. doi:10.1152/jappphysiol.00887.2016
- Lee, S. M. C., Feiveson, A. H., Stein, S., Stenger, M. B., and Platts, S. H. (2015). Orthostatic intolerance after ISS and space shuttle missions. *Aerosp. Med. Hum. Perform.* 86, A54. doi:10.3357/AMHP.EC08.2015
- Lee, S. M. C., Ribeiro, L. C., Martin, D. S., Zwart, S. R., Feiveson, A. H., Laurie, S. S., et al. (2020). Arterial structure and function during and after long-duration spaceflight. *J. Appl. Physiol.* 129, 108–123. doi:10.1152/jappphysiol.00550.2019
- Li, X.-T., Yang, C.-B., Zhu, Y.-S., Sun, J., Shi, F., Wang, Y.-C., et al. (2017). Moderate exercise based on artificial gravity preserves orthostatic tolerance and exercise capacity during short-term head-down bed rest. *Physiol. Res.* 66, 567–580. doi:10.33549/physiolres.933493
- Li, Y., Shi, H., Fan, Q., Bai, G., Duan, Y., and Xie, J. (2002). Effects of qiang gu kang wei compound on hemorheology in tail-suspended rats. *Hang Tian Yi Xue Yu Yi Xue Gong Cheng Space Med. Med. Eng.* 15, 327–330.
- Lillie, J. S., Liberson, A. S., Mix, D., Schwarz, K. Q., Chandra, A., Phillips, D. B., et al. (2015). Pulse wave velocity prediction and compliance assessment in elastic arterial segments. *Cardiovasc. Eng. Technol.* 6, 49–58. doi:10.1007/s13239-014-0202-x
- Lin, L.-J., Hsieh, N.-C., Wu, S.-F. V., Tan, T.-H., Alizargar, A., Bai, C.-H., et al. (2020). Factors associated with cardio ankle vascular index (CAVI) and its mathematically corrected formula (CAVI<sub>0</sub>) in community dwelling individuals. *Artery Res.* 27, 53–58. doi:10.2991/artres.k.201124.002
- Linnarsson, D., Hughson, R. L., Fraser, K. S., Clément, G., Karlsson, L. L., Mulder, E., et al. (2015). Effects of an artificial gravity countermeasure on orthostatic tolerance, blood volumes and aerobic power after short-term bed rest (BR-AG1). *J. Appl. Physiol.* 118, 29–35. doi:10.1152/jappphysiol.00061.2014
- Maggioli, M. A., Castiglioni, P., Merati, G., Brauns, K., Gunga, H.-C., Mendt, S., et al. (2018). High-intensity exercise mitigates cardiovascular deconditioning during long-duration bed rest. *Front. Physiol.* 9, 1553. doi:10.3389/fphys.2018.01553
- Mahmoudi, M., Farghadan, A., McConnell, D. R., Barker, A. J., Wentzel, J. J., Budoff, M. J., et al. (2020). The story of wall shear stress in coronary artery atherosclerosis: Biochemical transport and mechanotransduction. *J. Biomech. Eng.* 143, 041002. doi:10.1115/1.4049026
- Markl, M., Wallis, W., Strecker, C., Gladstone, B. P., Vach, W., and Harloff, A. (2012). Analysis of pulse wave velocity in the thoracic aorta by flow-sensitive four-dimensional MRI: Reproducibility and correlation with characteristics in patients with aortic atherosclerosis. *J. Magn. Reson. Imaging* 35, 1162–1168. doi:10.1002/jmri.22856
- Meloni, A., Zymeski, H., Pepe, A., Lombardi, M., and Wood, J. C. (2014). Robust estimation of pulse wave transit time using group delay. *J. Magn. Reson. Imaging* 39, 550–558. doi:10.1002/jmri.24207
- Moore, A. D., Downs, M. E., Lee, S. M. C., Feiveson, A. H., Knudsen, P., and Ploutz-Snyder, L. (2014). Peak exercise oxygen uptake during and following long-duration spaceflight. *J. Appl. Physiol.* 117, 231–238. doi:10.1152/jappphysiol.01251.2013
- Moran, V. H., Leathard, H. L., and Coley, J. (2000). Cardiovascular functioning during the menstrual cycle. *Clin. Physiol.* 20, 496–504. doi:10.1046/j.1365-2281.2000.00285.x
- Möstl, S., Orter, S., Hoffmann, F., Bachler, M., Hametner, B., Wassertheurer, S., et al. (2021). Limited effect of 60-days strict head down tilt bed rest on vascular aging. *Front. Physiol.* 12, 685473. doi:10.3389/fphys.2021.685473
- Navasolava, N., Yuan, M., Murphy, R., Robin, A., Coupé, M., Wang, L., et al. (2020). Vascular and microvascular dysfunction induced by microgravity and its analogs in humans: Mechanisms and countermeasures. *Front. Physiol.* 11, 952. doi:10.3389/fphys.2020.00952
- Nürnberg, J., Saez, A. O., Dammer, S., Mitchell, A., Wenzel, R. R., Philipp, T., et al. (2003). Left ventricular ejection time: a potential determinant of pulse wave velocity in young, healthy males. *J. Hypertens.* 21, 2125–2132. doi:10.1097/01.hjh.0000098125.00558.40
- Orter, S., Möstl, S., Bachler, M., Hoffmann, F., Mayer, C. C., Kaniusas, E., et al. (2022). A comparison between left ventricular ejection time measurement methods during physiological changes induced by simulated microgravity. *Exp. Physiol.* 107, 213–221. doi:10.1113/EP090103
- Onnis-Skali, N., Mitchell, G. F., Solomon, C. G., Solomon, S. D., and Seely, E. W. (2006). Changes in central arterial pressure waveforms during the normal menstrual cycle. *J. Investig. Med.* 54, 321–326. doi:10.2310/6650.2006.05055
- Palombo, C., Morizzo, C., Baluci, M., Lucini, D., Ricci, S., Biolo, G., et al. (2015). Large artery remodeling and dynamics following simulated microgravity by prolonged head-down tilt bed rest in humans. *Biomed. Res. Int.* 2015, e342565. doi:10.1155/2015/342565
- Pawelczyk, J. A., Zuckerman, J. H., Blomqvist, C. G., and Levine, B. D. (2001). Regulation of muscle sympathetic nerve activity after bed rest deconditioning. *Am. J. Physiol. Heart Circ. Physiol.* 280, H2230–H2239. doi:10.1152/ajpheart.2001.280.5.H2230
- Pedley, T. J. (Editor) (1980). *The fluid mechanics of large blood vessels* (Cambridge, UK: Cambridge University Press).
- Perhonen, M. A., Zuckerman, J. H., and Levine, B. D. (2001). Deterioration of left ventricular chamber performance after bed rest. *Circulation* 103, 1851–1857. doi:10.1161/01.CIR.103.14.1851
- Platts, S. H., Bairey Merz, C. N., Barr, Y., Fu, Q., Gulati, M., Hughson, R., et al. (2014). Effects of sex and gender on adaptation to space: Cardiovascular alterations. *J. Womens Health* 23, 950–955. doi:10.1089/jwh.2014.4912
- Platts, S. H., Martin, D. S., Stenger, M. B., Perez, S. A., Ribeiro, C. L., Summers, R., et al. (2009). Cardiovascular adaptations to long-duration head-down bed rest. *Aviat. Space Environ. Med.* 80, A29–A36. doi:10.3357/ASEM.BR03.2009
- Rabineau, J., Hossein, A., Landreani, F., Haut, B., Mulder, E., Luchitskaya, E., et al. (2020). Cardiovascular adaptation to simulated microgravity and countermeasure efficacy assessed by ballistocardiography and seismocardiography. *Sci. Rep.* 10, 17694. doi:10.1038/s41598-020-74150-5
- Ray, C. A., Vasques, M., Miller, T. A., Wilkerson, M. K., and Delp, M. D. (2001). Effect of short-term microgravity and long-term hindlimb unloading on rat cardiac mass and function. *J. Appl. Physiol.* 91, 1207–1213. doi:10.1152/jappphysiol.00191.3.1207
- Rikhtegar, F., Knight, J. A., Olgac, U., Saur, S. C., Poulikakos, D., Marshall, W., et al. (2012). Choosing the optimal wall shear parameter for the prediction of plaque location—a patient-specific computational study in human left coronary arteries. *Atherosclerosis* 221, 432–437. doi:10.1016/j.atherosclerosis.2012.01.018
- Ryou, M. (2003). Role of blood viscosity in the regulation of hematocrit in tail-suspended rats (*Rattus norvegicus*) treated with pentoxifylline. Available at: <https://eirc.emporia.edu/handle/123456789/1070> [Accessed May 9, 2022].
- Salvi, P., Palombo, C., Salvi, G. M., Labat, C., Parati, G., and Benetos, A. (2013). Left ventricular ejection time, not heart rate, is an independent correlate of aortic pulse wave velocity. *J. Appl. Physiol.* 115, 1610–1617. doi:10.1152/jappphysiol.00475.2013
- Saunders, D. K., Roberts, A. C., Aldrich, K. J., and Cuthbertson, B. (2002). Hematological and blood viscosity changes in tail-suspended rats. *Aviat. Space Environ. Med.* 73, 647–653.
- Shen, M., and Frishman, W. H. (2019). Effects of spaceflight on cardiovascular physiology and health. *Cardiol. Rev.* 27, 122–126. doi:10.1097/CRD.0000000000000236
- Shen, X., Dong, Q., Chen, J., Meng, J., Jin, Y., Wen, Z., et al. (1997). Erythrocyte deformation in simulated weightless human and rabbits. *J. Gravit. Physiol.* 4, 61–65.
- Shirai, K., Suzuki, K., Tsuda, S., Shimizu, K., Takata, M., Yamamoto, T., et al. (2019). Comparison of cardio-ankle vascular index (CAVI) and CAVI0 in large healthy and hypertensive populations. *J. Atheroscler. Thromb.* 26, 603–615. doi:10.5551/jat.48314
- Shirai, K., Utino, J., Otsuka, K., and Takata, M. (2006). A novel blood pressure-independent arterial wall stiffness parameter; cardio-ankle vascular index (CAVI). *J. Atheroscler. Thromb.* 13, 101–107. doi:10.5551/jat.13.101
- Soulis, J. V., Lampri, O. P., Fytanidis, D. K., and Giannoglou, G. D. (2011). “Relative residence time and oscillatory shear index of non-Newtonian flow models in aorta,” in 2011 10th International Workshop on Biomedical Engineering, Kos Island, 5–7 Oct. 2011, 1–4. doi:10.1109/IWBE.2011.6079011
- Spaak, J., Montmerle, S., Sundblad, P., and Linnarsson, D. (2005). Long-term bed rest-induced reductions in stroke volume during rest and exercise: cardiac

- dysfunction vs. volume depletion. *J. Appl. Physiol.* 98, 648–654. doi:10.1152/jappphysiol.01332.2003
- Spronck, B., Avolio, A. P., Tan, I., Butlin, M., Reesink, K. D., and Delhaas, T. (2017). Arterial stiffness index beta and cardio-ankle vascular index inherently depend on blood pressure but can be readily corrected. *J. Hypertens.* 35, 98–104. doi:10.1097/HJH.0000000000001132
- Spronck, B., Heusinkveld, M. H. G., Vanmolkot, F. H., Roodt, J. O. 't, Hermeling, E., Delhaas, T., et al. (2015). Pressure-dependence of arterial stiffness: potential clinical implications. *J. Hypertens.* 33, 330–338. doi:10.1097/HJH.0000000000000407
- Stalder, A. F., Russe, M. F., Frydrychowicz, A., Bock, J., Hennig, J., and Markl, M. (2008). Quantitative 2D and 3D phase contrast MRI: Optimized analysis of blood flow and vessel wall parameters. *Magn. Reson. Med.* 60, 1218–1231. doi:10.1002/mrm.21778
- Stankovic, Z., Allen, B. D., Garcia, J., Jarvis, K. B., and Markl, M. (2014). 4D flow imaging with MRI. *Cardiovasc. Diagn. Ther.* 4, 173–192. doi:10.3978/j.issn.2223-3652.2014.01.02
- Stenger, M. B., Evans, J. M., Knapp, C. F., Lee, S. M. C., Phillips, T. R., Perez, S. A., et al. (2012). Artificial gravity training reduces bed rest-induced cardiovascular deconditioning. *Eur. J. Appl. Physiol.* 112, 605–616. doi:10.1007/s00421-011-2005-1
- Stenger, M. B., Evans, J. M., Patwardhan, A. R., Moore, F. B., Hinghofer-Szalkay, H., Rössler, A., et al. (2007). Artificial gravity training improves orthostatic tolerance in ambulatory men and women. *Acta Astronaut.* 60, 267–272. doi:10.1016/j.actaastro.2006.08.008
- Sun, B., Zhang, L.-F., Gao, F., Ma, X.-W., Zhang, M.-L., Liu, J., et al. (2004). Daily short-period gravitation can prevent functional and structural changes in arteries of simulated microgravity rats. *J. Appl. Physiol.* 97, 1022–1031. doi:10.1152/jappphysiol.00188.2004
- Sun, X.-Q., Yao, Y.-J., Yang, C.-B., Jiang, S.-Z., Jiang, C.-L., and Liang, W.-B. (2005). Effect of lower-body negative pressure on cerebral blood flow velocity during 21 days head-down tilt bed rest. *Med. Sci. Monit.* 11, CR1–5.
- Takahashi, K., Yamamoto, T., Tsuda, S., Maruyama, M., and Shirai, K. (2020). The background of calculating CAVI: Lesson from the discrepancy between CAVI and CAV10. *Vasc. Health Risk Manag.* 16, 193–201. doi:10.2147/VHRM.S223330
- Takehara, Y. (2022). Clinical application of 4D flow MR imaging for the abdominal aorta. *Magn. Reson. Med. Sci.* 21, 354–364. doi:10.2463/mrms.rev.2021-0156
- Tanaka, K., Nishimura, N., and Kawai, Y. (2017). Adaptation to microgravity, deconditioning, and countermeasures. *J. Physiol. Sci.* 67, 271–281. doi:10.1007/s12576-016-0514-8
- Tang, B. T., Cheng, C. P., Draney, M. T., Wilson, N. M., Tsao, P. S., Herfkens, R. J., et al. (2006). Abdominal aortic hemodynamics in young healthy adults at rest and during lower limb exercise: quantification using image-based computer modeling. *Am. J. Physiol. Heart Circ. Physiol.* 291, H668–H676. doi:10.1152/ajpheart.01301.2005
- The Reference Values for Arterial Stiffness' Collaboration (2010). Determinants of pulse wave velocity in healthy people and in the presence of cardiovascular risk factors: 'establishing normal and reference values. *Eur. Heart J.* 31, 2338–2350. doi:10.1093/eurheartj/ehq165
- Thijssen, D. H. J., Green, D. J., and Hopman, M. T. E. (2011a). Blood vessel remodeling and physical inactivity in humans. *J. Appl. Physiol.* 111, 1836–1845. doi:10.1152/jappphysiol.00394.2011
- Thijssen, D. H. J., Scholten, R. R., van den Munckhof, I. C. L., Benda, N., Green, D. J., and Hopman, M. T. E. (2011b/1979). Acute change in vascular tone alters intima-media thickness. *Hypertension* 58, 240–246. doi:10.1161/HYPERTENSIONAHA.111.173583
- Traon, A. P., Vasseur, P., Arbeille, P., Güell, A., Bes, A., Gharib, C., et al. (1995). Effects of 28-day head-down tilt with and without countermeasures on lower body negative pressure responses. *Aviat. Space Environ. Med.* 66, 982–991.
- Trenti, C., Ziegler, M., Bjarnegård, N., Ebbens, T., Lindenberger, M., and Dyverfeldt, P. (2022). Wall shear stress and relative residence time as potential risk factors for abdominal aortic aneurysms in males: a 4D flow cardiovascular magnetic resonance case-control study. *J. Cardiovasc. Magn. Reson.* 24, 18. doi:10.1186/s12968-022-00848-2
- Tuday, E. C., Meck, J. V., Nyhan, D., Shoukas, A. A., and Berkowitz, D. E. (2007). Microgravity-induced changes in aortic stiffness and their role in orthostatic intolerance. *J. Appl. Physiol.* 102, 853–858. doi:10.1152/jappphysiol.00950.2006
- Tuday, E. C., Platt, S. H., Nyhan, D., Shoukas, A. A., and Berkowitz, D. E. (2011). A retrospective analysis on gender differences in the arterial stiffness response to microgravity exposure. *Gravitational Space Res.* 25. Available at: <http://gravitationalandspace-research.org/index.php/journal/article/view/533> (Accessed July 11, 2022).
- van der Palen, R. L. F., Roest, A. A. W., van den Boogaard, P. J., de Roos, A., Blom, N. A., and Westenberg, J. J. M. (2018). Scan-rescan reproducibility of segmental aortic wall shear stress as assessed by phase-specific segmentation with 4D flow MRI in healthy volunteers. *Magn. Reson. Mat. Phys. Biol. Med.* 31, 653–663. doi:10.1007/s10334-018-0688-6
- van Duijnhoven, N. T. L., Green, D. J., Felsenberg, D., Belavý, D. L., Hopman, M. T. E., and Thijssen, D. H. J. (2010). Impact of bed rest on conduit artery remodeling: effect of exercise countermeasures. *Hypertension* 56, 240–246. doi:10.1161/HYPERTENSIONAHA.110.152868
- van Hout, M. J., Scholte, A. J., Juffermans, J. F., Westenberg, J. J., Zhong, L., Zhou, X., et al. (2020). How to measure the aorta using MRI: A practical guide. *J. Magn. Reson. Imaging* 52, 971–977. doi:10.1002/jmri.27183
- Vernikos, J., Ludwig, D. A., Ertl, A. C., Wade, C. E., Keil, L., and O'Hara, D. (1996). Effect of standing or walking on physiological changes induced by head down bed rest: implications for spaceflight. *Aviat. Space Environ. Med.* 67, 1069–1079.
- Vlachopoulos, C., Aznaouridis, K., and Stefanadis, C. (2010). Prediction of cardiovascular events and all-cause mortality with arterial stiffness: a systematic review and meta-analysis. *J. Am. Coll. Cardiol.* 55, 1318–1327. doi:10.1016/j.jacc.2009.10.061
- Wang, Y.-C., Yang, C.-B., Wu, Y.-H., Gao, Y., Lu, D.-Y., Shi, F., et al. (2011). Artificial gravity with ergometric exercise as a countermeasure against cardiovascular deconditioning during 4 days of head-down bed rest in humans. *Eur. J. Appl. Physiol.* 111, 2315–2325. doi:10.1007/s00421-011-1866-7
- Watenpaugh, D. E., Ballard, R. E., Stout, M. S., Murthy, G., Whalen, R. T., and Hargens, A. R. (1994). Dynamic leg exercise improves tolerance to lower body negative pressure. *Aviat. Space Environ. Med.* 65, 412–418.
- Watenpaugh, D. E., and Hargens, A. R. (2011). "The cardiovascular system in microgravity," in *Comprehensive Physiology*. Editor R. Terjung (Hoboken, NJ, USA: John Wiley & Sons). doi:10.1002/cphy.cp040129
- Watenpaugh, D. E., O'Leary, D. D., Schneider, S. M., Lee, S. M. C., Macias, B. R., Tanaka, K., et al. (2007). Lower body negative pressure exercise plus brief postexercise lower body negative pressure improve post-bed rest orthostatic tolerance. *J. Appl. Physiol.* 103, 1964–1972. doi:10.1152/jappphysiol.00132.2007
- Waters, W. W., Ziegler, M. G., and Meck, J. V. (2002). Postspaceflight orthostatic hypotension occurs mostly in women and is predicted by low vascular resistance. *J. Appl. Physiol.* 92, 586–594. doi:10.1152/jappphysiol.00544.2001
- Wentland, A. L., Grist, T. M., and Wieben, O. (2013). Repeatability and internal consistency of abdominal 2D and 4D phase contrast MR flow measurements. *Acad. Radiol.* 20, 699–704. doi:10.1016/j.acra.2012.12.019
- Williams, B., Mancia, G., Spiering, W., Al, E., Bochud, M., Messerli, F., et al. (2018). 2018 ESC/ESH guidelines for the management of arterial hypertension: The task force for the management of arterial hypertension of the European society of cardiology and the European society of hypertension: The task force for the management of arterial hypertension of the European society of cardiology and the European society of hypertension. *J. Hypertens.* 36, 1953–2041. doi:10.1097/HJH.0000000000001940
- Williams, M. R., Westerman, R. A., Kingwell, B. A., Paige, J., Blombery, P. A., Sudhir, K., et al. (2001). Variations in endothelial function and arterial compliance during the menstrual cycle. *J. Clin. Endocrinol. Metab.* 86, 5389–5395. doi:10.1210/jcem.86.11.8013
- Xue, J.-H., Chen, L.-H., Zhao, H.-Z., Pu, Y.-D., Feng, H.-Z., Ma, Y.-G., et al. (2011). Differential regulation and recovery of intracellular Ca<sup>2+</sup> in cerebral and small mesenteric arterial smooth muscle cells of simulated microgravity rat. *PLOS ONE* 6, e19775. doi:10.1371/journal.pone.0019775
- Yang, C.-B., Wang, Y.-C., Gao, Y., Geng, J., Wu, Y.-H., Zhang, Y., et al. (2011). Artificial gravity with ergometric exercise preserves the cardiac, but not cerebrovascular, functions during 4 days of head-down bed rest. *Cytokine* 56, 648–655. doi:10.1016/j.cyt.2011.09.004
- Yang, C.-B., Zhang, S., Zhang, Y., Wang, B., Yao, Y.-J., Wang, Y.-C., et al. (2010). Combined short-arm centrifuge and aerobic exercise training improves cardiovascular function and physical working capacity in humans. *Med. Sci. Monit.* 16, CR575–83.
- Young, L. R., Hecht, H., Lyne, L. E., Sienko, K. H., Cheung, C. C., and Kavelaars, J. (2001). Artificial gravity: head movements during short-radius centrifugation. *Acta Astronaut.* 49, 215–226. doi:10.1016/S0094-5765(01)00100-X

Yuan, M., Alameddine, A., Coupé, M., Navasiolava, N. M., Li, Y., Gauquelin-Koch, G., et al. (2015). Effect of Chinese herbal medicine on vascular functions during 60-day head-down bed rest. *Eur. J. Appl. Physiol.* 115, 1975. doi:10.1007/s00421-015-3176-y

Zengin, K., Tokac, M., Duzenli, M. A., Soylu, A., Aygul, N., and Ozdemir, K. (2007). Influence of menstrual cycle on cardiac performance. *Maturitas* 58, 70–74. doi:10.1016/j.maturitas.2007.06.002

Zhang, B., Gu, J., Qian, M., Niu, L., Zhou, H., and Ghista, D. (2017). Correlation between quantitative analysis of wall shear stress and intima-media thickness in atherosclerosis development in carotid arteries. *Biomed. Eng. OnLine* 16, 137. doi:10.1186/s12938-017-0425-9

Zhang, L.-F. (2013). Region-specific vascular remodeling and its prevention by artificial gravity in weightless environment. *Eur. J. Appl. Physiol.* 113, 2873–2895. doi:10.1007/s00421-013-2597-8

Zhang, L.-F., Sun, B., Cao, X.-S., Liu, C., Yu, Z.-B., Zhang, L.-N., et al. (2003). Effectiveness of intermittent -Gx gravitation in preventing deconditioning due to simulated microgravity. *J. Appl. Physiol.* 95, 207–218. doi:10.1152/jappphysiol.00969.2002

Zhang, R., Zuckerman, J. H., Pawelczyk, J. A., and Levine, B. D. (1997). Effects of head-down-tilt bed rest on cerebral hemodynamics during orthostatic stress. *J. Appl. Physiol.* 83, 2139–2145. doi:10.1152/jappl.1997.83.6.2139

## Glossary

**AA** Ascending aorta

**AGBRESA** Artificial gravity bed rest with European space agency

**BDC** Baseline data collection

**AG** Continuous artificial gravity group

**cAG** Continuous artificial gravity group

**CAVI** Cardio-ankle vascular index

**CAVI<sub>0</sub>** Updated cardio-ankle vascular index

**CTRL** Control group

**CO<sub>low</sub>** Cardiac output allocated to the lower body

**CO<sub>tot</sub>** Total cardiac output

**CO<sub>up</sub>** Cardiac output allocated to the upper body

**DA** Descending aorta

**DBP** Diastolic blood pressure

**DLR** Deutsches Zentrum für Luft- und Raumfahrt (German aerospace center)

**ESA** European space agency

**g** Earth's gravitational acceleration

**HDT** Head-down tilt

**HR** Heart rate

**iAG** Intermittent artificial gravity group

**LVET** Left ventricular ejection time

**MRI** Magnetic resonance imaging

**n** Number of subjects

**NASA** National aeronautics and space administration

**NO** Nitric oxide

**OSI** Oscillatory shear index

**PTT** Pulse transit time

**PWV** Pulse wave velocity

**Q<sub>max,AA</sub>** Maximum blood flow rate in the ascending aorta

**Q<sub>max,DA</sub>** Maximum blood flow rate in the descending aorta

**R** Recovery

**RRT** Relative residence time

**SBP** Systolic blood pressure

**SV<sub>low</sub>** Stroke volume allocated to the lower body

**SV<sub>tot</sub>** Total stroke volume

**SV<sub>up</sub>** Stroke volume allocated to the upper body

**SVR** Systemic vascular resistance

**t** Time

**T** Duration of a cardiac cycle

**TAWSS** Time-averaged wall shear stress

**WSS** Wall shear stress

**WSS<sub>mean</sub>** Average amplitude of all the WSS reference points during the peak systolic phase

**%CO<sub>up</sub>** Percentage of cardiac output allocated to the upper body

**ρ** Volumetric mass density of blood